

QUANTUM TRANSMITTANCE

**THESIS SUBMITTED FOR THE DEGREE OF
DOCTOR OF PHILOSOPHY (SCIENCE)
OF
JADAVPUR UNIVERSITY
2002**

TAPAS MITRA

**Jadavpur University
Kolkata**

S. N. BOSE NATIONAL CENTRE FOR BASIC SCIENCES

JD Block, Sector 3, Salt Lake, Kolkata - 700 098

QUANTUM TRANSMITTANCE

**THESIS SUBMITTED FOR THE DEGREE OF
DOCTOR OF PHILOSOPHY (SCIENCE)
OF
JADAVPUR UNIVERSITY
2002**

TAPAS MITRA


**Jadavpur University
Kolkata**

S. N. BOSE NATIONAL CENTRE FOR BASIC SCIENCES

JD Block, Sector 3, Salt Lake, Kolkata - 700 098

CERTIFICATE

This is to certify that the thesis entitled **QUANTUM TRANSMITTANCE** submitted by Tapas Mitra for the award of Ph.D (Science) degree of Jadavpur University, India, is based upon his own work carried out under the supervision of Prof. Abhijit Mookerjee at S. N. Bose National Centre For Basic Sciences, Calcutta. Neither this thesis nor any part of it has been submitted for any degree/diploma or for any other academic award anywhere before.


ABHIJIT MOOKERJEE
Senior Professor,
Dean (Academic Programme),
Satyendranath Bose National Centre For Basic Sciences,
JD Block, Sector 3, Salt Lake City, Kolkata 700098
India
Date : 9/10/2002

अभिजित मुखर्जी / ABHIJIT MOOKERJEE
वरिष्ठ अध्यापक एवं अध्यक्ष (शि.का.) / Sr. Professor & Dean (A.P.)
एस.एन. बसु राष्ट्रीय मौलिक विज्ञान केन्द्र
S.N. Bose National Centre for Basic Sciences
साल्ट लेक, कोलकाता-700 098
Salt Lake, Kolkata - 700 098

Acknowledgments

I remember my late father for imparting a deep passion for knowledge in me. I express my gratitude to Prof. A. Mookerjee for excellent supervision and generous help and for teaching me the physics of disordered solids. I thank Dr. P. K. Thakur who was my collaborator in a significant portion of my research work. I should like to thank the late Prof. C.K. Majumdar for giving me the opportunity to work in the Centre. I thank the members of the staff of the S.N. Bose National Centre for Basic Sciences, Kolkata, where my research work was carried out, for their cooperation and help. I thank the members of the staff of the Saha Institute of Nuclear Physics, Kolkata for their support. I am grateful to all my teachers. My special thanks are for Prof. P. Dasgupta, Prof. P. Rudra and Dr. A.P. Chatterjee for their support and constant encouragement. I thank the authorities and the members of the staff of Ranaghat College, Ranaghat and Gurudas College, Kolkata for their cooperation. I thank the Council for Scientific and Industrial Research, Government of India for financial support. Finally, I wish to thank my family members for their constant support.

List of Publications

1. *Resonance pattern in electronic transmittance for two identical coupled random-dimer chains under different lead configurations*, Mitra T. and Thakur P.K., *Phys. Rev.* **B53** 9895 (1996)
2. *Characterization of the transmission resonances in different energy regimes by the multifractal scaling analysis of the electronic transmittance in a one-dimensional random dimer potential*, Thakur P.K. and Mitra T., *J. Phys.: Condens. Matter* **9** 8985 (1997)
3. *Electronic transmittance and localisation in quasi-1D systems of coupled identical n-mer chains*, Mitra T. and Thakur P.K., *Int. J. Mod. Phys. B* 1773 (1998)

Contents

1	Introduction	1
1.1	Introduction	1
1.2	The Measurement of Conductance	5
1.3	The Scattering formulation	9
1.4	Specific Models Studied	15
2	Effect of interchain coupling on transmittance in coupled random dimer chains	23
2.1	Introduction	23
2.2	Model of Two coupled Random-Dimer Chains	26
2.3	Vector Recursion Algorithm	27
2.4	Results and Discussion	32
2.5	Summary and Conclusion	40
3	Characterization of transmission resonances	42
3.1	Introduction	42
3.2	Electronic transmittance in the transfer matrix method	45
3.3	Multifractal Scaling	46
3.4	Results and Discussion	53
3.5	Summary and Conclusions	59
4	Electronic Transmittance and Localization in quasi-1d systems of coupled identical n-mer chains	61
4.1	Introduction.	61
4.2	Results and discussions	65
5	A Mode Based Formulation of the Vector Recursion Technique	69
5.1	Introduction	69
5.2	Formulation	71
5.2.1	The mode propagation picture	71
5.2.2	Mode-mode scattering	75

5.2.3	Vector recursion in a mode basis	78
5.3	Discussion	83

List of Figures

1.1	The Landauer scattering picture	6
2.1	Transmittance vs Energy for (a) $\epsilon_A=0.5$, $\epsilon_B=0.25$, $c=0.10$, $V_c=0.001$, $V=1.0$ and $N=2256$ sites. (b) $\epsilon_A=0.42$, $\epsilon_B=0.3$, $c=0.2$, $V_c=0.001$, $V=1.0$ and $N=3256$ sites.	33
2.2	Logarithm of Transmittance vs Energy for $\epsilon_A=0.5$, $\epsilon_B=0.25$, $c=0.10$, $V_c=0.35$, $V=1.0$ (a) $N=2256$ and (b) $N=3256$ sites.	35
2.3	Logarithm of Transmittance vs Energy for $\epsilon_A=0.42$, $\epsilon_B=0.3$, $c=0.2$, $V=1.0$ $N=2256$ (a) $V_c=0.125$ (b) $V_c=0.25$ and (c) $V_c=0.5$	36
2.4	Logarithm of Transmittance vs Energy for $\epsilon_A=0.42$, $\epsilon_B=0.3$, $c=0.2$, $V=1.0$ $N=3256$ $V_c=0.045$ (a) leads attached to corners (b) leads at- tached to two end of the lower lead.	38
2.5	Logarithm of Transmittance vs Energy for (a) $\epsilon_A=0.5$, $\epsilon_B=0.25$, $c=0.1$, $V=1.0$ $N=3256$ $V_c=1.0$ and (b) $\epsilon_A=0.42$, $\epsilon_B=0.3$, $c=0.2$, $V=1.0$ $N=3256$ $V_c=1.0$	39
3.1	Transmittance vs Energy for (a) $\epsilon_A=0.45$, $\epsilon_B=0.145$, $c=0.10$ and (a) $N=2 \times 10^3$ and (b) $N=2 \times 10^5$ sites. In this figure the upper graph has been vertically shifted by one unit in order to distinguish it from the one below	54
3.2	Transmittance vs Sample Size for the same set of parameters as figure 3.1 for (top) $E=0.452$ 28 (b) $E=0.472$ 16 and (c) $E=0.471$ 92 units. In this figure the upper graphs has been vertically shifted by one unit and two units respectively in order to distinguish it from the one below	55
3.3	The $f(\alpha)$ vs α curve for the same parameters as figure 3.1 for the state at (a) $E=0.452$ 28 (b) $E=0.472$ 16 (c) $E=0.47192$ units for $N=5 \times 10^4$ (bold), $N=1 \times 10^5$ (dashed) and $N=2 \times 10^5$ (dotted)	57

3.4	The $f(\alpha)$ vs α curve for $\epsilon_A = 0.15$, $\epsilon_B=0.045$ and $c=0.15$ for the state es at (a) $E=0.15246$ and (b) $E=0.18992$. The three curves are for same sizes as in figure 3.3	58
4.1	Transmittance vs Energy for $e_A = 0.01$ unit (host), $e_B = 0.11$ unit (impurity), $c=0.15$ (impurity concentration), $N=6000$ sites, and inter-chain couplings (solid,bottom) $V_c=0.15$ unit, (dashed, middle) $V_c=0.45$ unit and (dashed, top) $V_c=1.0$, for a case for two coupled 4-mer chains. The intrachain coupling in all cases was 1.0.	64
4.2	Transmittance vs Energy for $e_A = 0.01$ unit (host), $e_B = 0.11$ unit (impurity), $c=0.15$ (impurity concentration), (bottom) $N=2000$ sites, and (top) $N=6000$ sites. $V_c=1.0$, for a case for two coupled 4-mer chains. The intrachain coupling in all cases was 1.0.	66
4.3	Transmittance vs Energy for the same site energies for the host and the impurity and for the same impurity concentration as in the previous figure but for $V_c = 0.5$ unit and $N=6000$ sites (dashed) and $N=2000$ sites (solid) for a 4-mer in four chains.	67
5.1	A two-dimensional scatterer with two-dimensional leads	71
5.2	Some mode profiles along the finite section of a two-dimensional lead	73
5.3	An illustration of 'ghost' leads	74
5.4	A mode propagating along a lead	76
5.5	Scattering in a L-geometry and a Star-geometry	82

E R R A T A

1. The bottom sentence of page 21 and the top sentence of page 22 should be replaced by "This is why the method can be applied to the case where some leads are attached to intermediate positions of the samples (which are not necessarily on the two opposite ends), for example to the cases of 4 - leads systems ((Godin and Haydock (1988)), Gopar et al (1994), (Tarucha et al in Kirk and Reed (1992))).
2. Page 34, lines 11 and 12, the sentence "here the $\ln T$ vs E plot shows the growth whole energy region concerned" should be dropped.
3. Chapter 3, "vicinity" should be replaced by "vicinity of dimer on-site energy".

Chapter 1

Introduction

1.1 Introduction.

Studies of electronic eigenstates and their effect on the transport properties of systems where the potential has broken translational symmetry either because of disorder or incommensuration and inhomogeneity, have been the subject of a large body of work since the publication of Anderson's seminal paper in 1958 (Anderson (1958)). He showed that, contrary to the extended character of the electronic eigenstates in periodic potentials, under certain conditions, there is the possibility of localization of electronic eigenstates in random potentials. The degree of disorder is usually defined by a parameter Δ which measures the width of the probability distribution of potential parameters. The elastic mean free path level l_{el} , which at $T=0$ is the only characterization of scattering, is a function of Δ and depends on the dimension of the system.

For strong disorder Δ , the random potential scattering cuts off the wave function tail at some characteristic length ξ called the localization length. For such strong disorders, it is intuitively clear that the electron is contained within local wells. For very weak disorder it would seem plausible that the wavefunctions recover infinite

span, but this does not happen in one dimensional (1-D) and possibly in two dimensional (2-D) systems, of course, in absence of short-ranged correlation in the distribution of the potential parameters or applied external fields.

The importance of localization depends on the ratio of ξ to the sample length L . If $\xi \gg L$, then even though the impurity potential localizes the wavefunction (at least it would in an infinitely long sample of the same material), the measured dimensionless conductance $g \gg 1$, where $g = (h/e^2)G$, G being the conductance. In this case, even though the wavefunction spans the sample the conductance is still not impervious to localization. As the temperature T decreases, the coherence length L_ϕ for the wave-function increases. This happens because the electron rarely encounters a phase randomizing scattering by the phononic oscillations in the system. When $L_\phi \gg l_{el}$, the carrier has some likelihood of bouncing around and then returning back to its starting point. If phase coherence is maintained, the two sets of (time-reversed) paths clockwise and anti-clockwise around the loop of impurities interfere at the origin. The two partial waves arrive in phase (the path is of the same length in either direction so that $\phi_1 - \phi_2 = 0$) and interfere constructively. Constructive interference implies that less current flows away from the origin and the resistance rises. As the temperature, T , decreases and L_ϕ increases, loops of larger and larger circumference contribute to the interference and resistance increases Bergmann (1983). The mechanism is referred to as *weak localization* and the time-reversed pairs of paths are sometimes called *cooperons* because they bear formal similarity to superconducting pair excitations (Al'tshuler and Aronov (1985)). An applied external magnetic field reduces the effect of weak localization by destroying time-reversal symmetry. One standard method of obtaining transport co-efficients,

taking above mentioned quantum-mechanical corrections into consideration is that formulated by Kubo and Greenwood (Kubo (1956-7), Greenwood (1958)). The Kubo method underlies almost all of the perturbation calculations of conductance. Conductance calculated via Kubo's formula yields the Drude conductivity (which can be more directly obtained via classical Boltzmann transport Formalism) only if one assumes that the electron wavefunction is randomized between collisions with impurities. There is a parallel formulation by Landauer (Landauer (1970)), whose correspondence with the Kubo-Greenwood formula is described by Fisher and Lee (1981))

In the opposite limit, where the disorder is strong, $g \ll 1$ and the resistance tends to scale to infinity as $T \rightarrow 0$ and the sample tends to become an electrical insulator. In this regime of strong or Anderson localization, $l_{el}(\Delta, D) \simeq \lambda$ (where λ is the Fermi wavelength) and the electronic eigenstate corresponding to the Fermi Level is exponentially localized (the transmittance \mathbf{T} , discussed later is also exponentially localized). If the random potential is not strong enough then it cannot localize the states far away from the band edge to finite regions of space. Instead, the amplitude of the states, although fluctuating more or less randomly, will be non-zero essentially everywhere. Consequently, these states will be called extended. Within the energy region of extended states no localized states can exist. To see this, let us assume that there is a localized state in the extended region for some configuration of the disorder. Then by infinitesimally changing the disordered potential, a coupling between the localized and extended states is introduced and the localized state hybridizes with the extended states into new extended states. As a consequence two energies denoted by E_c and E'_c must exist within the spectrum separating the

extended from the localized states. Localized states do not contribute to transport even if they are situated at the Fermi Level, whereas extended states do. Thus E_c and E_c' are called *mobility edges*. In general, the mobility edges depend on the degree of disorder. If disorder Δ is large enough, then the mobility edges will merge into the centre of the band. The system becomes an insulator and the transition is called the Anderson Transition and is characterized by a critical value Δ_c of the disorder. $\Delta < \Delta_c$ means weak localization for at least some states and $\xi \rightarrow \infty$ that is the wave-function is not exponentially localized for those states¹. It is noteworthy that determination of the exact spatial nature of an electronic eigenstate has been attempted in various ways by numerous authors (see references in Chapter 3).

In the above discussion, the electron-electron interaction has been assumed to be negligible. This assumption is justified in many situations. It may be noted that, although previously it was thought that interaction enhances localization, in some recent works, electron interaction has been found to be responsible for delocalization in some situations (Shepelyanski (1994), Römer and Schreiber M. (1997), Evangelou *et al* (1996))

The study of electronic transport in translationally non-invariant systems has been going through a rapid advance since the eighties. On the one hand, this advance has been because of the fabrication of smaller and smaller samples from a wide variety of materials and the development of measurement techniques on these samples at very low temperatures. On the other hand, new theoretical concepts like universal conduction fluctuation and weak localization, new theoretical tools

¹Note, that this may not mean that the state is extended. It could be algebraically localized, for example

and availability of bigger and faster computers have facilitated the advance. One unforeseen benefit of this development that has started to emerge from the study of the small samples in the quantum mechanically coherent regime is that we are better able to understand some of the deep issues of quantum mechanics. We have experimentally seen the non-local nature of conductance and we now know what we measure depends upon how we measure it.

1.2 The Measurement of Conductance

Now I turn my attention to our work. We have attempted to study the steady-state electrical conductance by taking into account contributions of elementary quantum scattering events following Landauer approach and its generalizations (Landauer (1970)). In this formalism, perfectly conducting incoming and outgoing leads are attached to the sample. These leads serve as ‘*support space*’ for incoming and outgoing quantum states. In order to support asymptotically free-from-scattering incoming and outgoing quantum states, the leads have to be free of scattering centres and hence must be considered perfect conductors.

The scattering approach to the motion of electrons in disordered conductors, pioneered by Landauer, expresses the conductance solely in terms of the total transmission coefficients of the sample, considered as a single, complex scattering center. We summarize here briefly the arguments leading to the simplest expression of this type, which applies to the ideal two-probe conductance measurement (Imry (1986)) described below.

We note that any derivation of this type is to some extent heuristic, because no theorist had attempted to model the full complex interaction Hamiltonian cor-

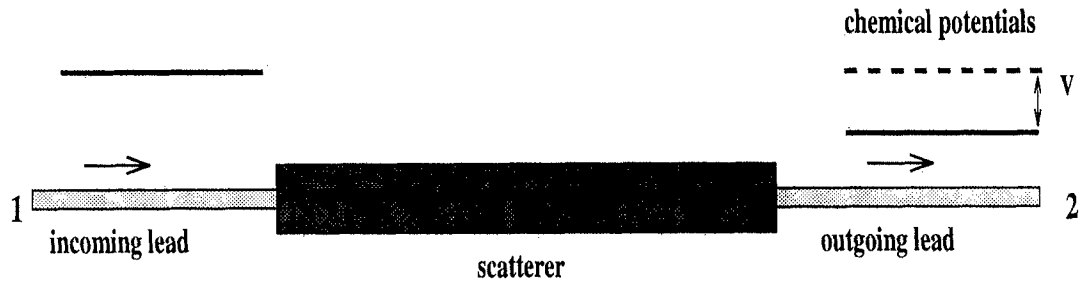


Figure 1.1: The Landauer scattering picture

responding to an experimental resistance measurement.

An ideal two-probe measurement is one in which the sample is attached between two perfect reservoirs with electro-chemical potentials, μ_1 and $\mu_2 = \mu_1 + eV$ respectively (where V is the applied voltage) and these reservoirs serve both as current source and sink and as voltage terminals. A perfect reservoir is defined to have the following properties:

1. It is initially in equilibrium at electro-chemical potential μ and this equilibrium is negligibly disturbed by the current flow.
2. Particles entering the reservoirs never return without loss of phase memory.
3. The connection between the reservoir and the sample generates no additional resistance.

Because of the imbalance of chemical potentials current will flow from reservoir 1 to 2. The total current which flows can be obtained from a *counting argument*. In the energy interval eV between μ_2 and μ_1 electrons are injected into right-going states emerging from reservoir 1, but none are injected into left-going states emerging from reservoir 2. Thus there is a net right-going current proportional to the number of states in the interval $\mu_1 - \mu_2$, given by

$$\begin{aligned}
I &= e \sum_i^N v_i \frac{dn_i}{d\varepsilon} eV \sum_j^N T_{ij} \\
&= \left[(e^2/h) \sum_{ij}^N T_{ij} \right] V
\end{aligned} \tag{1.1}$$

where N is the number of propagating channels in the sample, v_i is the longitudinal velocity for the i -th momentum channel at the Fermi surface, T_{ij} is the transmission probability from j to i , and we have used the fact that for a quasi-1D density of states, $dn_i/d\varepsilon = (1/h)v_i$.

If we assume that the conductance is measured by dividing the induced current by the chemical potential difference between two regions *deep within the reservoirs* (where by assumption equilibrium is negligibly disturbed), then equation (1.1) yields an expression for the two-probe conductance, g (measured in units of e^2/h),

$$g = \sum_{ij}^N T_{ij} = \text{Tr}[\mathbf{t}\mathbf{t}^\dagger] \tag{1.2}$$

where \mathbf{t} is the transmission matrix, a sub-matrix of the scattering S-matrix whose standard definition is given below. Thus the two-probe conductance is expressible solely in terms of the eigenvalues of the matrix $\mathbf{t}\mathbf{t}^\dagger$, but note that these eigenvalues are not simply related to those of the complete scattering S-matrix (which are modulus unity and mix up reflecting and transmitting channels).

Equation (1.2) can also be obtained from a more formal derivation from quantum linear response theory (Fisher and Lee (1981), Stone and Szafer (1988), Baranger and Stone (1989)), except that the heuristic construction of perfect reservoirs is hidden in the choice of boundary conditions : the reservoirs are replaced by semi-

infinite perfect leads at fixed potentials. A useful intermediate result in such a derivation is that the two-probe conductance is given by the flux of the conductivity tensor through the two surfaces connecting the sample to the leads,

$$g = \int \int dS_1 \cdot \sigma(x_1, x_2) \cdot dS_2$$

this expression can be transformed using the integral equation of scattering theory to yield equation (1.2). Since the conductivity tensor for a non-interacting system is given by the well-known expression involving the energies and current matrix elements of the exact eigenstates (Baranger and Stone (1989)), this emphasizes that the conductance is *not* determined solely by the eigenvalues of the Hamiltonian. Therefore we find the approach developed below more natural and potentially more powerful than arguments applying random matrix theory to the ensemble of disordered Hamiltonians. Nonetheless, Al'tschuler and Shklovskii (1986) have certainly given further insight into the origin of the universal conductance fluctuations using the latter approach combined with microscopic calculations.

The two-probe conductance measurement described by equation (1.2) does correspond reasonably well to one common type of experimental measurement, even in the limit of zero disorder in which it predicts a *quantized contact resistance* (Imry (1986)) very similar to that recently observed experimentally (van Wees *et al* (1988), Wharam *et al* (1988)). It was assumed in the derivation of equation (1.2) that the current through the sample and the voltage across the sample are measured at the same reservoir. However, the majority of experiments performed on mesoscopic conductors are so-called four-probe measurements in which a current is injected from a source into a sink, and the voltage induced *across the sample* is

measured by separate voltage probes connected with a separate pair of reservoirs. This is done to avoid contact resistance and other spurious effects. It is now clear that the behaviour in this situation can differ substantially from the predicted by equation (1.1), particularly when the voltage probes are spaced much less than an inelastic scattering length apart, and an adequate extension of the theory (Stone and Szafer (1988)), based upon a *multi-probe Landauer formula* (Büttiker *et al* (1985), Landauer (1970)) has recently been developed.

However for the general questions addressed here, relating to the minimal physical assumptions necessary to generate the universal statistical properties of disordered conductors, we do not need to consider the additional complications introduced by the multi-probe approach. Moreover, in the more general theory, the fundamental statistical quantities are still moments of the transmission matrix, so that the information obtained from the two-probe theory should still be of relevance in that context. Extensions of our approach to the multi-probe situation have not yet been made. We do however remind the reader of the necessity of using the multi-probe theory if one wishes to obtain a quantitative description (or even in some cases qualitative agreement) with many experiments on mesoscopic conductors.

1.3 The Scattering formulation²

We have just seen that the calculation of the quantum-mechanical conductance is equivalent to the calculation of the transmission matrix t through a disordered medium. The disordered medium generates multiple scattering, and the full scatter-

²The contents of this portion has been described by Stone *et al* in Al'tschuler *et al* (1991)

ing S-matrix must describe these complex scattering processes. Unfortunately, the scattering S-matrix itself does not satisfy a simple composition rule which allows one to easily determine the full scattering S-matrix if that describing a single scattering event is known. Therefore we consider a different but related matrix, the transfer matrix \mathbf{M} , which has a simple multiplicative composition rule. We shall see below that this approach has both computational and conceptual advantages. We now define these quantities carefully for the system of interest, disordered conductors with only elastic scattering from the random potential.

Employing the two-probe model described above, we imagine the disordered system of interest to be placed between two semi-infinite perfectly conducting leads of finite width. We assume the existence of boundary conditions at the transverse surfaces which quantize the energy of the transverse part of the wavefunction; the theory is not sensitive to the detailed nature of the boundary conditions and so we take them to be infinite hard-walls for definiteness. Then in the perfect conductors, the scattering states at the Fermi energy satisfy the relation $k_f^2 = k_n^2 + k^2$, where k_f is the Fermi momentum, k the longitudinal momentum and k_n the quantized transverse momentum. The various $k_n (n = 1, \dots, N)$, which satisfy this relation such that $k^2 > 0$ define the N channels. Since each channel can carry two waves traveling in opposite directions, the wave function on either side of the disordered region is specified by a $2N$ - component vector: the first N components are the amplitudes of the waves propagating to the right, and the remaining N components are the amplitudes of the waves traveling to the left. The scattering matrix \mathbf{S} relates the incoming flux to the outgoing flux

$$\mathbf{S} \begin{pmatrix} I \\ I' \end{pmatrix} = \begin{pmatrix} O \\ O' \end{pmatrix} \quad (1.3)$$

where I, O, I', O' are the N -component vectors describing the wave amplitudes on left and right, respectively. In this quasi-one-dimensional geometry, the scattering S-matrix is a $2N \times 2N$ matrix of the form

$$\mathbf{S} = \begin{pmatrix} \mathbf{r} & \mathbf{t} \\ \mathbf{t}' & \mathbf{r}' \end{pmatrix} \quad (1.4)$$

where \mathbf{t} is the $N \times N$ transmission matrix which yields the conductance in equation (1.2) and \mathbf{r} is the $N \times N$ reflection matrix. (Throughout this work we shall frequently represent $2N \times 2N$ in terms of their $N \times N$ blocks, hence all 2×2 matrices with boldface entries will represent $N \times N$ block decompositions of $2N \times 2N$ matrices.) Current conservation implies that

$$|I|^2 + |I'|^2 = |O|^2 + |O'|^2 \quad (1.5)$$

which is equivalent to the unitarity of the scattering S-matrix.

Although the scattering S-matrix determines the conductance through equation (1.2), it does not satisfy a simple composition rule suitable for introducing a scaling approach. Therefore, we instead consider the transfer matrix which contains the same information in a different form.

By definition, the $2N \times 2N$ transfer matrix \mathbf{M} relates the flux amplitudes on the left-hand side of the disordered region to those on the right,

$$\mathbf{M} \begin{pmatrix} I \\ O \end{pmatrix} = \begin{pmatrix} O' \\ I' \end{pmatrix} \quad (1.6)$$

Just as with \mathbf{S} , we can write \mathbf{M} in terms of four $N \times N$ blocks

$$\mathbf{M} = \begin{pmatrix} \mathbf{m}_1 & \mathbf{m}_2 \\ \mathbf{m}_3 & \mathbf{m}_4 \end{pmatrix} \quad (1.7)$$

and from the definitions (1.3), (1.4) and (1.6) one finds the relations

$$\begin{aligned} \mathbf{m}_1 &= (\mathbf{t}^\dagger)^{-1} & \mathbf{m}_2 &= \mathbf{r}'(\mathbf{t}')^{-1} \\ \mathbf{m}_3 &= -(\mathbf{t}')^{-1}\mathbf{r} & \mathbf{m}_4 &= (\mathbf{t}')^{-1} \\ \mathbf{t} &= (\mathbf{m}_1^\dagger)^{-1} & \mathbf{r} &= \mathbf{m}_4^{-1}\mathbf{m}_3 \end{aligned}$$

The flux conservation constraint on the transfer matrix is easily found by re-expressing equation (1.5) in the form

$$|I|^2 - |O|^2 = |O'|^2 - |I'|^2 \quad (1.8)$$

which means from equation (1.5) that \mathbf{M} preserves the *hyperbolic* norm of the vector $\begin{pmatrix} I \\ O \end{pmatrix}$. This defines a $U(N, N)$ (*pseudo-unitary*) matrix. An alternative way of expressing the flux conservation constraint on \mathbf{M} is

$$\mathbf{M}^\dagger \Sigma_z \mathbf{M} = \Sigma_z$$

or equivalently,

$$\mathbf{M} \Sigma_z \mathbf{M}^\dagger = \Sigma_z \quad (1.9)$$

Here Σ_z denotes the matrix

$$\Sigma_z = \begin{pmatrix} \mathbf{I} & \mathbf{0} \\ \mathbf{0} & -\mathbf{I} \end{pmatrix}$$

Here and below $\mathbf{1}$ designates the unit matrix, which will be either $2N \times 2N$ or $N \times N$ depending on context, and $\Sigma_i, i = x, y, z$ denotes the $2N \times 2N$ analog of the Pauli matrices satisfying $\varepsilon_{ijk} \Sigma_i \Sigma_j = i \Sigma_k, \Sigma_i^2 = \mathbf{I}$. We see that the requirement of flux conservation implies that the transfer matrices, \mathbf{M} , form a pseudo-unitary group $U(N, N); I_2 = (2N)^2$ is the number of independent parameters specifying such a matrix, just as for the more familiar unitary group $U(2N)$. If the Hamiltonian governing the system is invariant under the operation of time-reversal and we neglect spin (as we shall do throughout), then a second solution to equation (1.6) is obtained by interchanging incoming and outgoing channels and complex conjugating the wave function amplitudes. This implies that our transfer matrices \mathbf{M} must also satisfy the requirement

$$\mathbf{M}^* = \Sigma_x \mathbf{M} \Sigma_x \quad (1.10)$$

where

$$\Sigma_x = \begin{pmatrix} \mathbf{0} & \mathbf{I} \\ \mathbf{I} & \mathbf{0} \end{pmatrix}$$

To implement this further constraint, we could perform a unitary transformation on each \mathbf{M} of the form

$$\mathbf{P} = \mathbf{U}_s^\dagger \mathbf{M} \mathbf{U}_s \quad (1.11)$$

where

$$\mathbf{U}_s = \frac{1}{\sqrt{2}} \begin{pmatrix} \mathbf{I} & -\mathbf{i} \\ -\mathbf{i} & \mathbf{I} \end{pmatrix}$$

It is easy to show that the new matrices \mathbf{P} satisfy the relation $\mathbf{P}^\dagger \mathbf{J} \mathbf{P} = \mathbf{J}$, where,

$$\mathbf{J} = -\mathbf{i}\Sigma_y = \begin{pmatrix} \mathbf{0} & -\mathbf{I} \\ \mathbf{I} & \mathbf{0} \end{pmatrix}$$

This means that the matrices \mathbf{P} are symplectic. This mapping from $U(N, N)$ becomes useful in the presence of time-reversal symmetry since it can be checked that the condition (1.10) on \mathbf{M} implies that the \mathbf{P} matrices of equation (1.11) must be real, $\mathbf{P} = \mathbf{P}^*$, i.e. they form a real symplectic group $SP(2N, \mathbb{R})$, which is specified by $I_1 = N(2N+1)$ parameters. This mapping to the real symplectic group was used by Muttalib *et al* (1987) and Mello *et al* (1988). It has the advantage of simplifying the time-reversal symmetry constraint used in the derivation of the relevant invariant measures, but the disadvantage of introducing a new set of matrices with no simple physical interpretation³. We shall not use this mapping in the present work. Transfer matrices \mathbf{M} with time-reversal symmetry, i.e. satisfying both equations (1.9) and (1.10), are the relevant quantities to study when the sample is not a subject to a magnetic field, and the scattering is spin-independent. This case is analogous to the well-studied *orthogonal* ensembles (Dyson (1962), Mehta (1967), Brody *et al* (1981)) and is characterized by a symmetry parameter $\beta = 1$. If a magnetic field is present, time-reversal symmetry is broken and our transfer matrices satisfy the

³Note, the matrix \mathbf{P} here is not to be confused with the *real-space* transfer matrix which connects the real-space wavefunction amplitudes on either side of the disordered region. The latter matrix has a dimension equal to the number of lattice sites in the transverse direction, whereas the former has a dimension equal to N , the number of propagating channels. In general, these two dimensions are not equal.

requirement (1.9) alone; this case is analogous to the *unitary* ($\beta = 2$) ensembles (Dyson (1962)). The origin of this terminology and of the parameter β which measures the strength of the statistical correlations (level repulsion) in the ensemble (Dyson (1962)) will be explained shortly, when we review the properties of the standard ensembles. Throughout this work we will assume exact spin degeneracy of the channels, and therefore only mention briefly the effect of spin-orbit scattering which leads to the third and final universality class, the *symplectic* ensemble ($\beta = 4$). For the ensemble of disordered conductors, this case has been studied thoroughly by Zanon and Pichard (1988), and it shows the behaviour expected by the standard extrapolation from the orthogonal and unitary cases discussed here.

The correspondence between the Kubo formalism mentioned earlier and the Landauer approach has been discussed by Lee and Fisher (Fisher and Lee (1981)).

I now focus my attention to the specific topics that I have studied.

1.4 Specific Models Studied

Mott and Twose (1961), Borland (1961) and later Ishii (1973), in a more rigorous work, showed that almost all electronic eigenstates of a one-dimensional random potential are localized, even if the randomness is infinitesimally small. Localization takes place because of coherent multiple backscattering of electrons by the random variations of the potential. Later, it was found there some zero-measure configuration dependent extended states, randomly situated in the energy spectrum, (Azbel (1983-84), Azbel and Soven (1983), Basu *et al* (1991)).

However, these zero-measure states do not contribute to conductance in real

systems due to the fact that these states have zero-width. Conducting states in real material must have some width due to the finite life-time arising from the presence of different scattering agents. The scaling theory of Abrahams *et al* (1979) confirmed that almost all electronic eigenstates are localized in one dimension even in the presence of infinitesimal disorder. In these studies, the Renormalization Group Technique was used, the conductance was considered to be the only scaling variable and it was shown that disorder turns a one dimensional solid into an insulator. Numerical calculations also supported this view (Ramakrishnan and Lee (1985)). However in all these studies mentioned above, it was assumed that there was no spatial correlation between the randomness at different sites. The introduction of a correlation in the randomness of potential at different sites might make the single parameter inadequate for the purpose of scaling because of the introduction of another length scale in the Hamiltonian. However, people overlooked this limitation and consequently there was surprise when it was shown that, if there is short range correlation in the random potential, a regime of extended electronic states existed on the spectrum and various models were studied in this context (see the footnote 2 of chapter 2). Among all the models studied so far, the Random-Dimer Model (RDM) has gained special importance since Wu and Phillips (1991) showed that it has a direct connection with the anomalous electrical conductivity in polymers of the kind of the polyaniline. RDM is a particular type of Anderson's Tight Binding Hamiltonian (TBH). Since its introduction by Anderson (1958), TBH has been used widely in the literature of electronic states in disordered solids to capture the essence of physics in these systems. The TBH is written as,

$$H = \sum_i e_i |i\rangle\langle j| + \sum_{ij} V_{ij} |i\rangle\langle j|$$

We shall take $V_{ij} \neq 0$ only for nearest neighbours. Here $|i\rangle$ is a localized basis, localized at the i -th atomic the e 's are called the *site-energies* and V 's are called the *hopping* terms. As a wave-function at time t is given by $\psi(t) = \exp\{-(i/\hbar)Ht\} \psi(0)$, V_{ij} causes electrons to hop to adjacent sites. So a TBH describes a solid as an array of potential wells and an electron in a well has a finite probability of tunnelling to adjacent wells. For a periodic solid, e 's and V 's are same throughout the solid and the eigenstates are Bloch states which form a band of a width proportional to \surd .

Now a Random Dimer Model is a TBH where impurity site energies occur in pairs in the host. We shall take, the hopping term V_{ij} to be the same for all the sites. Let us consider the stationary state solution of a TBH \hat{H} having energy E ,

$$\hat{H}|\phi\rangle = E|\phi\rangle$$

If

$$|\phi\rangle = \sum_m \phi_m |m\rangle$$

then projections ϕ_m of the state $|\phi\rangle$ on the site-labelled bases, $|m\rangle$, satisfy the following relation if we consider the 1-D case,

$$\begin{bmatrix} \psi_{m+1} \\ \psi_m \end{bmatrix} = M(m) \begin{bmatrix} \psi_m \\ \psi_{m-1} \end{bmatrix}$$

Here the matrix $M(m)$ is called the Transfer Matrix and is given by

$$M(m) = \begin{bmatrix} (E - e_m)/V & -1 \\ 1 & 0 \end{bmatrix}$$

where V is the nearest neighbour hopping term taken to be constant throughout the chain.

In the particular case of the RDM, pairs of impurity atoms having site energies e_{imp} are injected randomly in the host having site energy e_p . It is seen that $M^2 = \hat{I}$ when $E = e_{imp}$ so an extended state will be obtained with the energy eigen-value E it lies within the band of the host. For the one-dimensional chain, the band of the host extends from the energy value $e_p - 2V$ to $e_p + 2V$. It is to be noted that we analytically obtain this extended state for one particular value $E = e_{imp}$. The system will show metallic property if the Fermi Energy of the system coincides with this energy and also, as discussed earlier, the state must have some finite width i.e. a number of states around that energy have also to be non-scattered around the energy. Although there is no analytical result for the existence of these states a few studies have indicated the existence of these non-scattered states (Wu and Phillips (1991), Wu *et al* (1992), Phillips *et al* (1990), Dunlap *et al* (1989)) .

All the studies described above have been done in the context of one-dimensional RDM which is the correct description of the polyaniline systems if the contribution from the sideways coupling between individual chains is neglected. Wu and Phillips (1991) have pointed towards the necessity of taking the coupling from sideways into account in the the consideration of conductance of real world polyaniline systems. There had been no analytical or numerical result on the effect of finite inter-chain coupling on the resonance pattern of one-dimensional RDM before we looked into the problem.

In the Chapter 2, we have studied the outstanding and important issue of whether and how the resonance pattern of 1-D RDM model survives under the presence of

finite inter-chain coupling. We have used the Vector Recursion Method (Godin and Haydock (1988), Godon and Haydock (1991), which was previously shown to be numerically stable in 1-D, 2-D and 3-D systems (Basu *et al* (1991), Dasgupta *et al* (1992), Saha *et al* (1994)) to calculate electronic transmittance.

I have already mentioned of the necessity of the existence of extended states which have finite width for the observation of metallic behaviour in a system. So the determination of the nature of the resonance states in the Random Dimer Model is a matter of immense interest. We have used the formalism of Multifractal Analysis for this purpose in Chapter 3. It is to be noted that extended states (which have finite width), exponentially localized states, Resonance states having zero measure (of zero width) and the states which are neither extended nor exponentially localized behave differently under Multifractal Analysis (Fujiwara *et al* (1989), Schreiber and Grussbach (1991), Basu *et al* (1991), Thakur *et al* (1992), Grussbach and Schreiber (1993), Basu and Thakur (1995), Yakubo and Goto (1996)) A noteworthy feature of our way of doing Multifractal Analysis is that we have used normalized transmittance which is directly observable (since it is related to the conductance through Landauer Formalism) as our measure. This way of doing Multifractal Analysis has been previously applied successfully to distinguish between electronic states of different types (Basu *et al* (1991), Thakur *et al* (1992), Basu and Thakur (1995))

Random n -mer Models are generalizations of the Random Dimer Model. 1-D Random n -mer model is an Anderson's Tight Binding Hamiltonian where the impurity site energy ϵ_A occur in blocks containing n number of sites and these blocks are injected randomly into the host sample having site energy ϵ_B . The hopping parameter V is taken to be constant throughout the sample. It has been shown recently

that there are at least $(n - 1)$ number extended states in 1-D Random n -mer models provided that the energies of these are within the band of the host (Sil *et al* (1993), Chen and Xiong (1993)). The energies of these extended states are given by

$$E_l = \epsilon_A + 2V \cos\left(\frac{l\pi}{n}\right) \quad l = 1, 2 \dots n - 1$$

It has been shown using the properties of 2×2 unimodular matrices that at these energy values the transfer matrix M given by

$$\hat{M} = \begin{pmatrix} (E - \epsilon_A)/V & -1 \\ 1 & 0 \end{pmatrix}$$

satisfy the following relation. $M^n = (-1)^l \hat{I}$ where \hat{I} is the identity matrix. Since the matrix $(-1)^l \hat{I}$ has no effect on the amplitudes of the wave function, we get an extended state provided E_l is within the range from $\epsilon_B - 2V$ upto $\epsilon_B + 2V$. In Chapter 4 we have studied the effect of finite inter-chain coupling an electronic transmittance pattern in quasi-1D systems where impurity blocks of the types (i) **AAAA** and (ii) **AAA** are present. The Vector Recursion method has been used for calculating electronic transmittance. It is to be noted that the results for Random n -mer models can be verified by fabricating appropriate layered hetero-junction and by coupling quantum dots (Giri *et al* (1993)). Recently Bellani *et al* (1999) have built random dimer superlattices and have seen the inhibition of localization and formation of extended states.

Our studies may be important for designing new quantum devices due to the possibility of merger of several resonances and for understanding the anomalous electrical conductivity in polyaniline and other related systems.

Recently there has been considerable development in the field of micro lithogra-

phy and layer growth technique of semiconductor quantum heterostructures. These developments have made it possible to develop systems that have characteristic scales less than the phase coherence length l_ϕ and the small size of these structures greatly reduces the defect scattering. The motion of electrons in these systems is similar to that of the electro-magnetic waves in waveguides. In these systems, both changes of shapes of the samples and defects in the underlying potential the important sources of scattering. The interplay of these two types of scattering is the essence of the physics of electronic transmittance in these systems. Studying electronic transmittance of these samples of different shapes is an important field of research. This investigation may lead to the development of new quantum interference devices, like quantum transistors, which are analogous to the corresponding optical devices. Also important quantum mechanical phenomena like quantization of conductance and Bohm-Aharonov oscillation in these systems. Studying of electronic transmittance in these systems is also important from the point of view of quantum manifestation of classical chaos.

In chapter 5, we develop a new formalism for calculating electronic transmittance in these samples. We generalize the vector recursion method in this formalism and we consider the 3-dimensional character of the incoming and the outgoing leads. With this formalism we are able to calculate elegantly the total transmittance and reflectance. A distinct advantage of this formalism is that the states which are known exactly to match the boundary conditions are included a priori in the basis. This is why the method can be applied to the case where some leads are attached to intermediate positions of the samples (which are not necessary in the two opposite

ends). As an example, waves from two perpendicular direction enter the sample⁷⁴ and to the 4-leads systems are discussed in the reference number [75-76]. Another distinct advantage of this formalism is that it is applicable even to the case where the long-range hopping is non zero.

Acknowledgement

The following reviews proved invaluable sources for the ideas expressed in this chapter :

- Lee P. and Ramakrishnan T.V., *Rev. Mod. Phys.* **57** 287 (1985)
- *Mesoscopic Phenomenon in Solids* edited by A. L. Altshuller, P.A. Lee and R.A. Webb (North Holland, Amsterdam) (1991)
- Washburn S. and Webb R.A., *Rep. Prog. Phys.* **55** 1311 (1992)
- *A course on many-body theory applied to Solid State Physics*, C.P. Enz (World Scientific 1992)
- Kramer B. and McKinnon A., *Rep. Prog. Phys.* **56** 1469 (1993)

Chapter 2

Effect of interchain coupling on transmittance in coupled random dimer chains¹

2.1 Introduction

Electronic states in random potentials were known to be localized both in one and two dimensions even for infinitesimally small disorder (See Mott and Twose (1961), Borland (1961), Ishii (1973), Ramakrishnan and Lee (1985)). However, in the past Azbel and Soven (1983), Pendry (1987) and Basu *et al* (1991) have reported the existence of extended states appearing in the form of exponentially narrow resonances in electronic transmission through random potentials at energy points randomly positioned in the spectrum. But these zero-measure states do not contribute to the conductance. In recent years much effort has been devoted to the study of electronic transport in disordered systems which have some kind of short-range correlation in the potential ² In these works the existence of extended states in

¹This chapter is partly based on the published paper : Mitra and Thakur, *Phys. Rev.* **B53** 9895 (1996)

²Dunlap *et al* (1989), Dunlap *et al* (1990), Phillips *et al* (1990), Wu and Phillips (1991), Wu *et al* (1992), Sil *et al* (1993), Gangopadhyay and Sen (1992), Datta *et al* (1993), Giri *et al* (1993), Sanchez

a disordered potential in one dimension with a short-ranged spatial correlation is predicted, in contrast to the all-states-localized situation for a random potential without any spatial correlation. In this context many models have been proposed to describe some realistic situation, as one can have, for example, in the transport mechanism for conducting polymers (Dunlap *et al* (1989), Dunlap *et al* (1990), Wu and Phillips (1991), Wu *et al* (1992), Phillips *et al* (1990)) or quasi-one-dimensional (quasi-1D) superlattices (Sanchez (1994), Hilke (1994), Ducker *et al* (1992), Stafstrom (1995), Progodin and Efetov (1993)). The simplest of these models is the random-dimer model (RDM) of Dunlap *et al* (1990). It has been shown by Wu and Phillips (1991) that a single protonated strand of conducting polymeric polyaniline can be described by the RDM. Recently, attempts have been made to describe the electronic transport mechanism in some super-lattice structures by Krönig-Penny-type models for random-dimer potentials (Sanchez (1994)). It has been realized that RDM's support a band of non-scattered states which can account for the enhanced conductivity in these materials (Wu and Phillips (1991), Wu *et al* (1992), Phillips *et al* (1990)). It has been shown that delocalization, even in the dense defect limit, arises from the single-impurity resonance effect and eventually forms a broad resonance of finite width (where transmittance is unity) around the dimer defect resonance energy. However, the detailed numerical calculation by Datta *et al* (1993) for finite concentrations of dimer defects have shown that the width is sensitive to the choice of site energies and concentration. In all these physically relevant systems, in which randomness as well as some short-ranged correlation is present, it was hoped that transport would be dominant only in one direction. Thus the result of the

(1994), Soukoulis *et al* (1994), Basu and Thakur (1995), Chen and Xiong (1993), Heinrichs (1995).

one-dimensional Hamiltonian was thought to be sufficient to describe the physical situation one observes in polyaniline or in other relevant systems. However, the idea of modeling a real system by coupled chains with small inter-chain coupling or by an effectively decoupled single chains may break down in some situations. Wu and Phillips (1991) think that the dynamics will be inherently two dimensional if the transverse hopping distance is comparable to the single-chain length. This chapter addresses an important outstanding issue with the random dimer model, namely the role of interchain coupling. This is a key issue that should be resolved in the application of the dimer model to conducting polymers. The effect of electron tunneling in the transverse direction may become important in general in many realistic quasi-1D systems³.

It is to be noted that nowadays it has been possible to build nanoscale materials with intentional and short-ranged correlated disorder and Bellani *et al* (1999) have found the inhibition of localization and formation of extended states in random dimer superlattices.

This motivated us to study electronic transport in a system of two coupled random chains with short-range correlation with the RDM. As we will see, our investigation will throw some light on transport characteristics influenced by the inter-chain hopping contributions. The idea is to check, for small or moderate values of inter-chain hopping, whether the resonant features within a broad band are really preserved. We will also investigate whether different localization-delocalization behaviour may set in due to the same inter-chain tunneling but with different lead configurations.

³Hilke (1994),Ducker *et al* (1992),Stafstrom (1995),Progodin and Efetov (1993)

2.2 Model of Two coupled Random-Dimer Chains

Here we describe the electron motion in a geometry of two coupled chains, by an Anderson tight-binding Hamiltonian. The Hamiltonian can be written as

$$\hat{H} = \sum_{n=-\infty}^{+\infty} (\mathbf{P}_n^\dagger \epsilon_n \mathbf{P}_n + \mathbf{P}_n^\dagger \mathbf{V}_{n,n+1} \mathbf{P}_{n+1} + \mathbf{P}_{n+1}^\dagger \mathbf{V}_{n+1,n} \mathbf{P}_n) \quad (2.1)$$

where ϵ_n , $\mathbf{V}_{n,n+1}$, and \mathbf{P}_n are the following matrices with site and chain indices:

$$\epsilon_n = \begin{pmatrix} \epsilon_n^1 & V_c \\ V_c & \epsilon_n^2 \end{pmatrix},$$

$$\mathbf{V}_{n,n+1} = \begin{pmatrix} t_{n,n+1}^1 & 0 \\ 0 & t_{n,n+1}^2 \end{pmatrix} = \mathbf{V}_{n+1,n},$$

$$\mathbf{P}_n = \begin{pmatrix} |n^1\rangle \\ |n^2\rangle \end{pmatrix}$$

The superscripts 1 and 2 refer to the two chains.

The two chains have been considered to be identical. Thus here an arrangement of sites in a single chain is all that is necessary. We generate the random-dimer model by assigning the site energy to a pair, called a dimer, distributed randomly along the chain. The site energy ϵ_n^1 is selected from the value generated from a random number sequence ($0 < R < 1$) in the following way: If $R < c$, then

$$\epsilon_n^{1,2} = \epsilon_{n+1}^{1,2} = \epsilon_A,$$

while for, $R > c$,

$$\epsilon_n^{1,2} = \epsilon_{n+1}^{1,2} = \epsilon_B$$

where c is a fraction between 0 and 1.

This is a quasi-1D system, where short-ranged correlation is due to the block of four impurity sites, and the inter-chain hopping V_c is considered to be finite in contrast to the decoupled random-dimer chain where a pair of sites occupied by the same species produces short-ranged correlation. The model of two identical coupled random-dimer chains simulates a quasi-1D wire where the impurity atoms appear within a block in the host.

We focus our main interest to the regime $V_c \leq V$, which constitutes a different physically distinct regime as compared to the decoupled chain limit, *i.e.* $V_c \ll V$.

2.3 Vector Recursion Algorithm

We employ the vector recursion algorithm of Godin and Haydock (1988) to calculate quantum electronic transmittance. This method has also been used elsewhere by Basu *et al* (1991), Dasgupta *et al* (1992) and Saha *et al* (1994) and has proven to be numerically stable in 1D, 2D, and 3D systems. The Hamiltonian of the sample is usually taken to be a tight-binding model, where only nearest-neighbour overlaps are nonzero. We attach M number of 1D incoming leads on one side of the sample, and M number of 1D outgoing leads on the opposite side of the sample. The Hamiltonian of the perfectly conducting leads is :

$$\hat{H}_L = V_L \sum_i \sum_j |i\rangle \langle j| \quad (2.2)$$

V_L can be adjusted to make the lead bandwidth comparable to or larger than that of the sample. These leads support incoming and outgoing waves into and away from the sample.

The aim of the method is to calculate transmittance and reflectance (which are related to the square modulus of non-diagonal and diagonal elements of the S-matrix, S , for the stationary state problem

$$\hat{H}|\psi\rangle = E|\psi\rangle \quad (2.3)$$

In this method, a basis is calculated recursively in which the sample Hamiltonian becomes block tridiagonal, i.e., if we partition the sample Hamiltonian into matrix blocks of size $2M \times 2M$ then only diagonal and sub-diagonal blocks are nonzero. The lead Hamiltonian is kept unchanged. The first element $|\phi_1\rangle$ of this basis is chosen to be

$$|\phi_1\rangle = \begin{bmatrix} u_1^I \\ u_2^I \\ \vdots \\ u_M^I \\ u_{M+1}^O \\ u_{2M+1}^O \\ \vdots \\ u_{2M}^O \end{bmatrix}$$

where u 's refer to those orbitals of the samples where leads are attached. Here I and O refer to incoming and outgoing channels. Subsequent elements of the basis are generated from the following relations:

$$\begin{aligned} B_2^+|\phi_2\rangle &= (\hat{H} - A_1)|\phi_1\rangle \\ B_{n+1}^+|\phi_{n+1}\rangle &= (\hat{H} - A_n)|\phi_n\rangle - B_n|\phi_{n-1}\rangle \end{aligned} \quad (2.4)$$

for $n \geq 2$.

If the original basis of the sample containing N orbitals was represented by N row vectors of size N , then the basis is represented by matrices of size $2M \times N$. A_n 's and B_n 's are $2M \times 2M$ matrices,

$$\begin{aligned}
A_n &= \langle \phi_n^\dagger | \hat{H} | \phi_n \rangle \\
B_n &= \langle \phi_{n+1}^\dagger | \hat{H} | \phi_n \rangle \\
B_1 &= \text{diag}(V_L, V_L, \dots, V_L)
\end{aligned}$$

The solution of the stationary-state problem in equation (2.3) within the sample is given by

$$|\Psi\rangle = \sum_n \psi_n |\phi_n\rangle$$

The projections ψ_n 's of the stationary-state solution $|\Psi\rangle$ into the basis $\{|\phi_n\rangle\}$ is calculated from the relation

$$\begin{aligned}
\psi_n &= X_n \psi_0 + Y_n \psi_1 \\
\text{where } |\phi_0\rangle &= \begin{bmatrix} u_1^{I'} \\ u_2^{I'} \\ \vdots \\ u_M^{I'} \\ u_{M+1}^0 \\ \vdots \\ u_{2M}^0 \end{bmatrix}
\end{aligned}$$

and u^0 's and $u^{I'}$'s refer to the orbitals at M outgoing and incoming lead ends (respectively) coupled to the sample via matrix element V_L . ψ_0 is the projection of Ψ into $|\phi_0\rangle$. X_n 's and Y_n 's are $2M \times 2M$ matrices calculated by the same recursion relation that was used to calculate the basis, with EI replacing the Hamiltonian \hat{H} and with the initial choices, $X_0 = \hat{I}$, $Y_0 = \hat{0}$, $X_1 = \hat{0}$, and $Y_1 = \hat{I}$. X 's and Y 's and $\hat{0}$ and \hat{I} are $2M \times 2M$ matrices.

As the sample basis space is of rank N , our basis is spanned by $N/2M = p$ independent elements. This leads to the boundary condition

$$\psi_{p+1} = X_{p+1}\psi_0 + Y_{p+1}\psi_1 = 0 \quad (2.5)$$

The solution of equation(2.3) in the leads are Bloch waves of the form

$$\psi_L = \sum_m A e^{\pm im\theta} |m\rangle \quad (2.6)$$

where θ is the relative phase between the projections of ψ_L into the m th and $(m+1)$ th site orbitals of the leads, and $\cos \theta = E/2V_L$. The second boundary condition comes from the known solution in the leads,

$$\psi_m = \begin{pmatrix} e^{im\theta} + r_{1,1}e^{-im\theta} + r_{1,2}e^{-im\theta} + \dots + r_{1,M}e^{-im\theta} \\ e^{im\theta} + r_{2,1}e^{-im\theta} + r_{2,2}e^{-im\theta} + \dots + r_{2,M}e^{-im\theta} \\ \vdots \\ t_{M+1,1}e^{im\theta} + t_{M+1,2}e^{im\theta} + \dots + t_{M+1,M}e^{im\theta} \\ t_{M+2,1}e^{im\theta} + t_{M+2,2}e^{im\theta} + \dots + t_{M+2,M}e^{im\theta} \\ \vdots \\ t_{2M,1}e^{im\theta} + t_{2M,2}e^{im\theta} + \dots + t_{2M,M}e^{im\theta} \end{pmatrix} \quad (2.7)$$

m being 0 or 1. Here r stands for the reflection coefficient, and t stands for the transmission coefficient. If we now interchange the incoming and outgoing leads we obtain another set of boundary conditions.

$$\psi'_m = \begin{pmatrix} t_{1,M+1}e^{-im\theta} + t_{1,M+2}e^{-im\theta} + \dots + t_{1,2M}e^{-im\theta} \\ t_{2,M+1}e^{-im\theta} + t_{2,M+2}e^{-im\theta} + \dots + t_{2,2M}e^{-im\theta} \\ \vdots \\ t_{M,M+1}e^{-im\theta} + t_{M,M+2}e^{-im\theta} + \dots + t_{M,2M}e^{-im\theta} \\ e^{-im\theta} + r_{M+1,M+1}e^{im\theta} + r_{M+1,M+2}e^{im\theta} + \dots + r_{M+1,2M}e^{im\theta} \\ e^{-im\theta} + r_{M+2,M+1}e^{im\theta} + r_{M+2,M+2}e^{im\theta} + \dots + r_{M+2,2M}e^{im\theta} \\ \vdots \\ e^{-im\theta} + r_{2M,M+1}e^{im\theta} + r_{2M,M+2}e^{im\theta} + \dots + r_{2M,2M}e^{im\theta} \end{pmatrix} \quad (2.8)$$

m is 0 or 1.

and

$$\psi'_{p+1} = X_{p+1}\psi'_0 + Y_{p+1}\psi'_1 = 0 \quad (2.9)$$

From the boundary conditions written in expressions (2.5-2.9), we obtain the expression for the S matrix:

$$S = \begin{pmatrix} r & t \\ t' & r' \end{pmatrix} = -[X_{p+1} + Y_{p+1} \exp(-i\theta)]^{-1} [X_{p+1} + Y_{p+1} \exp(i\theta)] \quad (2.10)$$

The total transmittance and reflectance are given by

$$\begin{aligned} T &= \sum_I \sum_O \left| \frac{t_{OI}}{2M} \right|^2 \\ R &= \sum_I \sum_{I'} |r_{II'}/2M|^2 \end{aligned} \quad (2.11)$$

Here we have $R + T = 1$ due to current conservation. Furthermore, as there is no applied magnetic field, the time-reversal symmetry holds good, and so $S_{ij} = S_{ji}$.

The relation between conductance and transmittance has been obtained in many contexts regarding both single-channel and multi-channel situations, either from the Kubo-Greenwood formula or from the Landauer formula (Kubo (1956-7), Greenwood (1958), Fisher and Lee (1981), Landauer (1970)).

2.4 Results and Discussion

In our calculations we have chosen the site energy in the lead Hamiltonian to be zero and the intra-chain hopping in the leads and the sample to be unity. The inter-chain hopping of the sample is small for $V_c \ll V$, and large when V_c becomes of the order of V .

We have studied the total transmittance (T) for the two coupled random-dimer chains with the same hopping V along the chains and different choices of the site energies ϵ , i.e., (ϵ_A, ϵ_B) , and concentration (c) of dimer impurities in the chains. We first choose a set of parameters $\epsilon_A = 0.5, \epsilon_B = 0.25, c = 0.10$, and $V_c = 0.001$ for the calculation of transmittance for a wide range of energies, namely from -1.0 to 1.5 in units of hopping parameters in the lead Hamiltonian. First we attach two decoupled 1D leads on either side of each chain, that is, the calculation is done in the four-lead geometry. In figures (2.1 a and b) T vs energy (E) is plotted for the first set of parameters for a system size $N = 3256$ sites. One can clearly see that for a wide range of energy values around $E = 0.50$ the transmittance becomes almost flat, i.e., ($T \sim 1$). We can consider this value of V_c to be small enough to produce the single random-dimer chain result. This is indicative of the fact that there are extended states, which is at least true for such finite sample sizes.

We do the calculations for another set of parameters, i.e. $\epsilon_A = 0.42, \epsilon_B =$

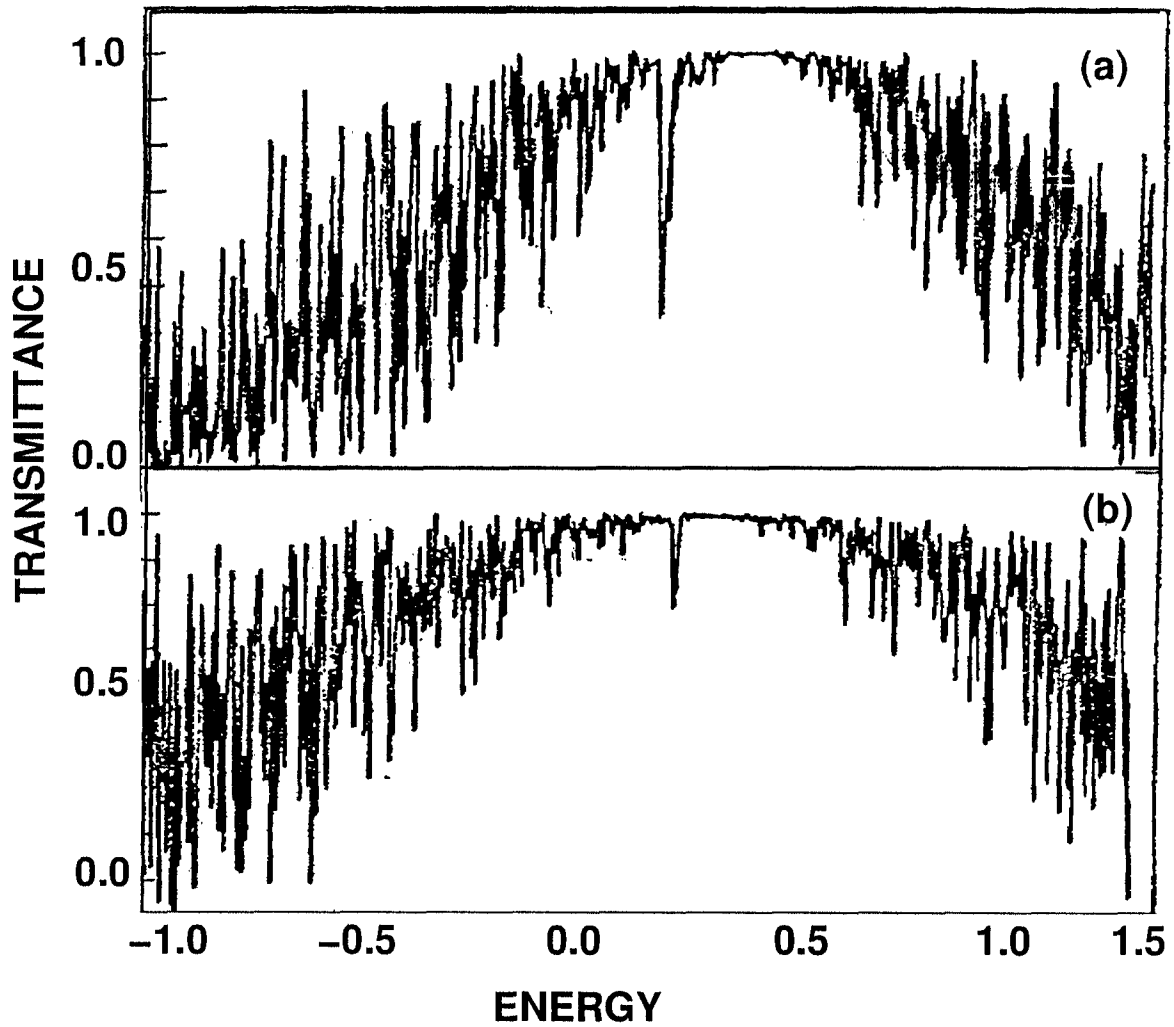


Figure 2.1: Transmittance vs Energy for (a) $\epsilon_A=0.5$, $\epsilon_B=0.25$, $c=0.10$, $V_c=0.001$, $V=1.0$ and $N=3256$ sites. (b) $\epsilon_A=0.42$, $\epsilon_B=0.3$, $c=0.2$, $V_c=0.001$, $V=1.0$ and $N=3256$ sites.

0.30, $V_c = 0.001$, $c = 0.20$, and $N = 3256$ sites. The transmittance T vs energy plot for this case is shown in figure 2.1(b), clearly showing again the single-chain dimer result, i.e., the existence of non-scattered states for a range of energy values around $E = 0.42$.

Next we choose the inter-chain hopping parameter V_c to be comparatively large, to make the electron motion in the transverse direction significant so that transport characteristics change from the strictly 1D situation. We calculate the transmittance for $\epsilon_A = 0.5$, $\epsilon_B = 0.25$, $c = 0.10$, and $V_c = 0.25$, for two different system sizes $N = 2256$ and 3256 sites. In figure 2.2 the $\ln T$ vs E plot is shown for two different sizes. One can hardly distinguish the two curves since the resonant features do not change much with the increase of system size. Here the $\ln T$ vs E plot shows the growth of $\ln T$ from the left or right of the whole energy region concerned. It has a different delocalization nature for the states having $\ln T \sim 0$ than the non-scattered state one observes in figures 2.1 (a) and (b). The regime of energies where $\ln T \sim 0$ corresponds to states with large localization lengths.

Now we go to a regime of transverse hopping, where the parameter $V_c = 0.125$, 0.25 , and 0.50 for $\epsilon_A = 0.42$, $\epsilon_B = 0.30$, $c = 0.20$, and $N = 2256$ sites. Transmittance versus energy graphs have been shown in figures 2.3 (a)-(c), for these parameters, and in the four-lead geometry as before. Here the input and output leads are attached to the ends along the chain direction. As before, we have studied the $\ln T$ vs energy E plot for finite chain coupling V_c . In this situation, the motion of electrons in the transverse direction also becomes significant and the total transmittance gives a clear signature of the combined interference effects due to the motion of electrons along the chain direction as well as in the transverse direction. Thus, with the in-

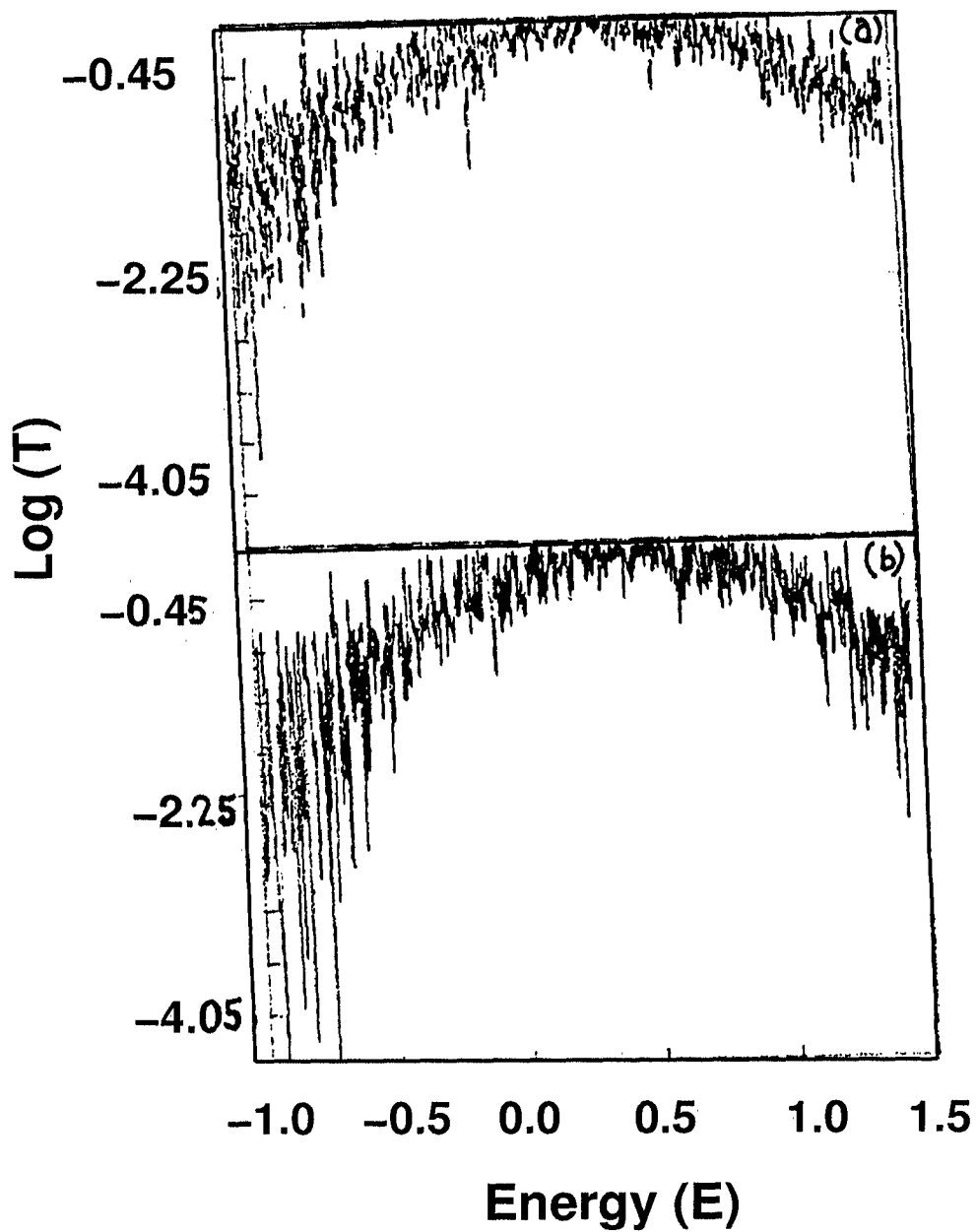


Figure 2.2: Logarithm of Transmittance vs Energy for $\epsilon_A = 0.5$, $\epsilon_B = 0.25$, $c = 0.1$, $V_c = 0.25$ and (a) $N = 2256$ (b) $N = 3256$ sites.

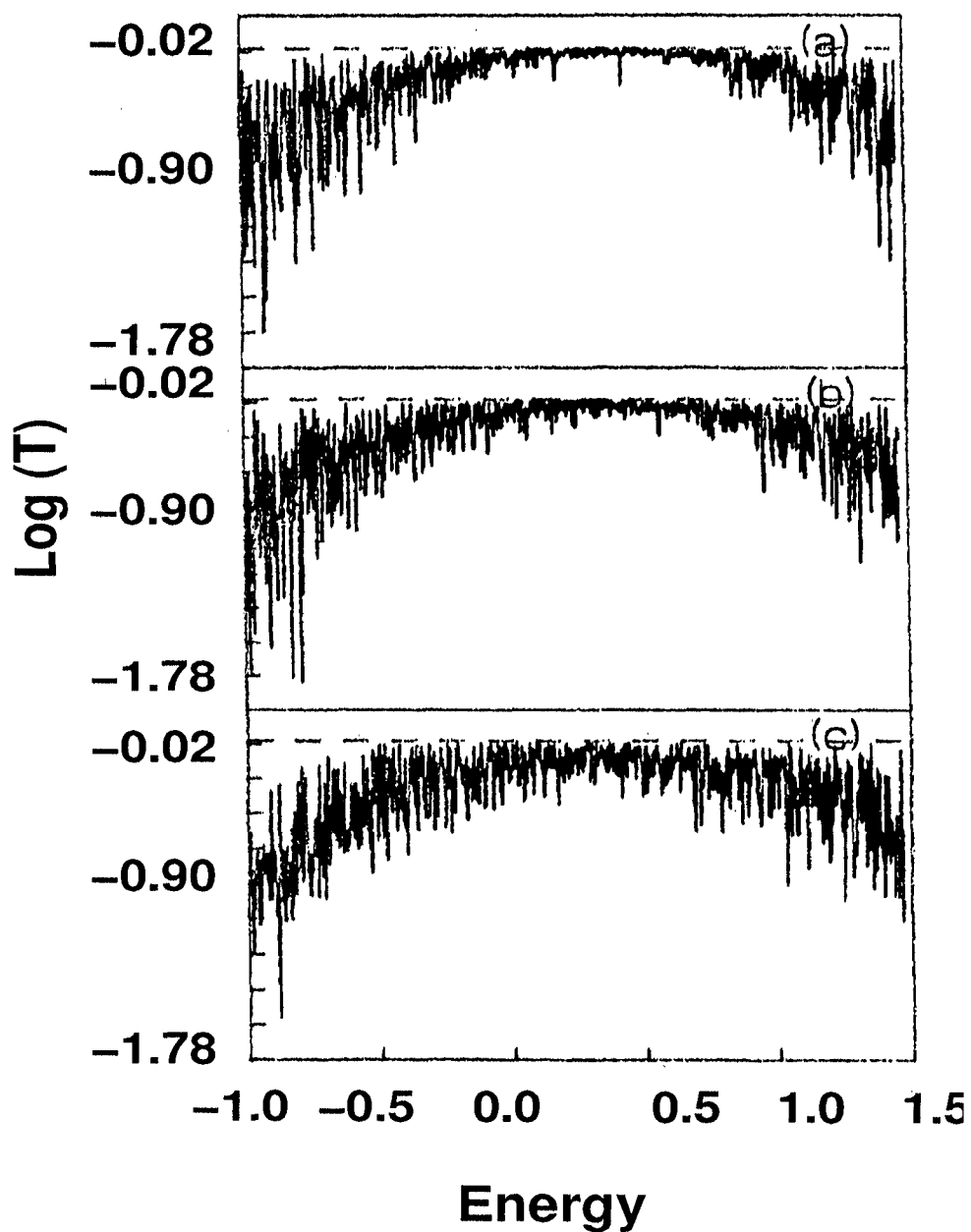


Figure 2.3: Logarithm of Transmittance vs Energy for $\epsilon_A=0.42$, $\epsilon_B=0.3$, $c=0.2$, $V=1$, $N=2256$ and (a) $V_c=0.125$ (b) $V_c=0.25$ (c) $V_c=0.5$

crease of inter-chain hopping parameters from 0.125 to 0.50, the overall resonance features in the transmittance drastically changes to a fluctuating pattern over all energy scales. In the resonant region (where $\ln T \sim 0$) it shows almost uniform fluctuations. Thus for a wide range of energies, the delocalization of states is manifested as before, with an underlying fluctuation pattern in contrast to the extended states (transmittance is flat and $T \rightarrow 1.0$) in the single random-dimer chain. Now we will analyze situations where electronic transmittance has been calculated in different measurement geometries and where, for the first case, the input and output leads are at the corners of the sample, and for the second, they are on the two sides of a single chain. We see how resonance features may become different in such different input-output lead configurations. In fig.4(a) a transmittance vs energy plot has been shown when input and output leads are at the corners and the inter-chain coupling V_c is finite; here we choose $V_c = 0.045$. However, the other chain parameters are the same as in figures 2.3 (a)-(c) but the system size is $N = 3256$ sites.

Figure 2.4(b) shows the same plot but with input-output leads attached to the left and right sides of the lower chain respectively, for the same set of parameters as in figure 2.4(a). If we compare figures 2.4 (a) and (b) we find that different nature of the localization-delocalization aspects have been reflected through the $\ln T$ vs E curve for the same sample but with different lead configurations. In both figures the $\ln T$ vs. E plot gives a clear signature for regions of many delocalized states as well as sharp dips which occur in an irregular fashion. As we see increasing the coupling V_c will lead to more and more dips appearing in an irregular fashion in the vicinity of states having $\ln T \sim 0$. This is attributable to the underlying quantum interference effects under different lead configurations.

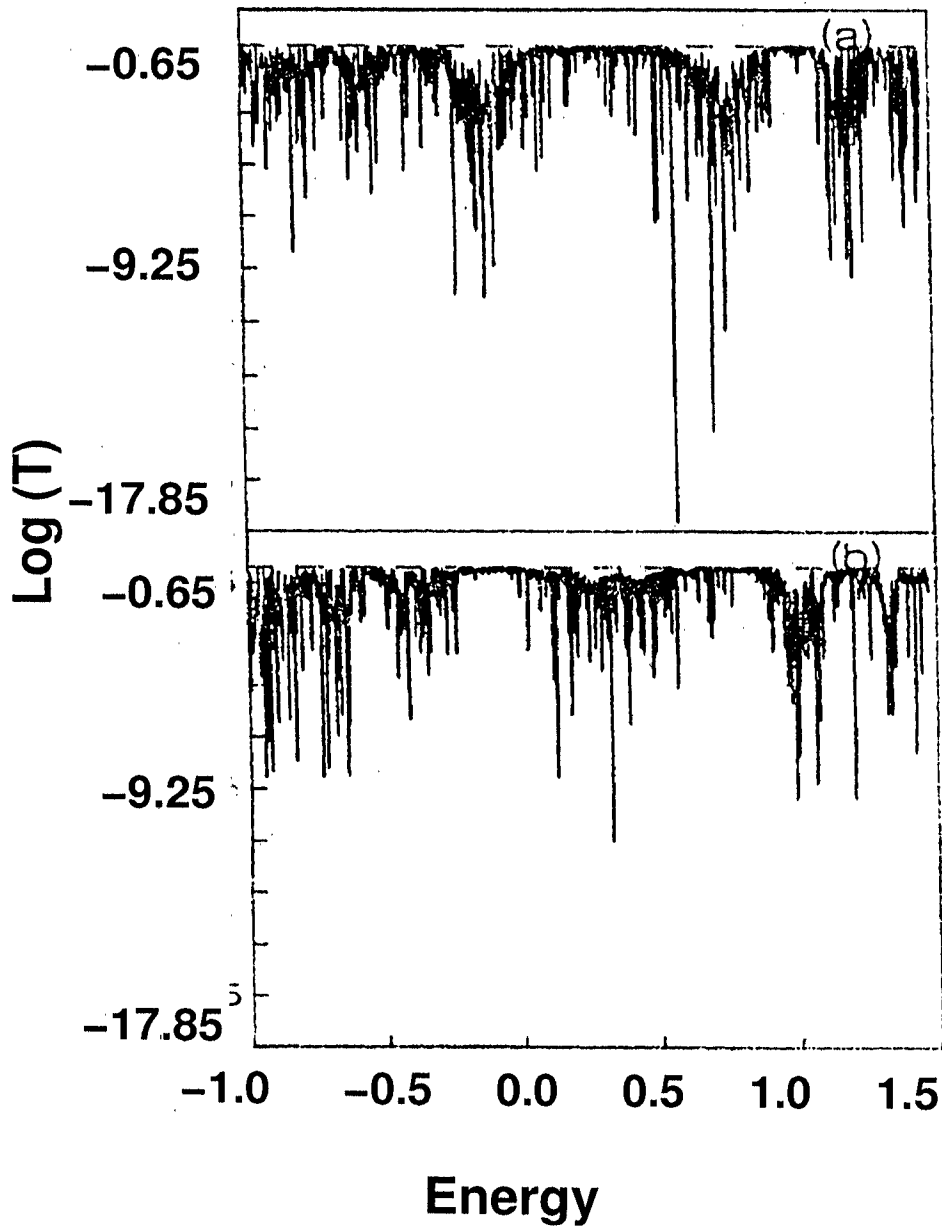


Figure 2.4: (a) Logarithm of Transmittance vs Energy for corner leads attached to a sample for chain parameters as in figure 2.3(a) but for $V_c=0.045$ and $N=3256$ (b) Same as (a) but for the situation where the leads are attached on the left and right ends of the lower chain.

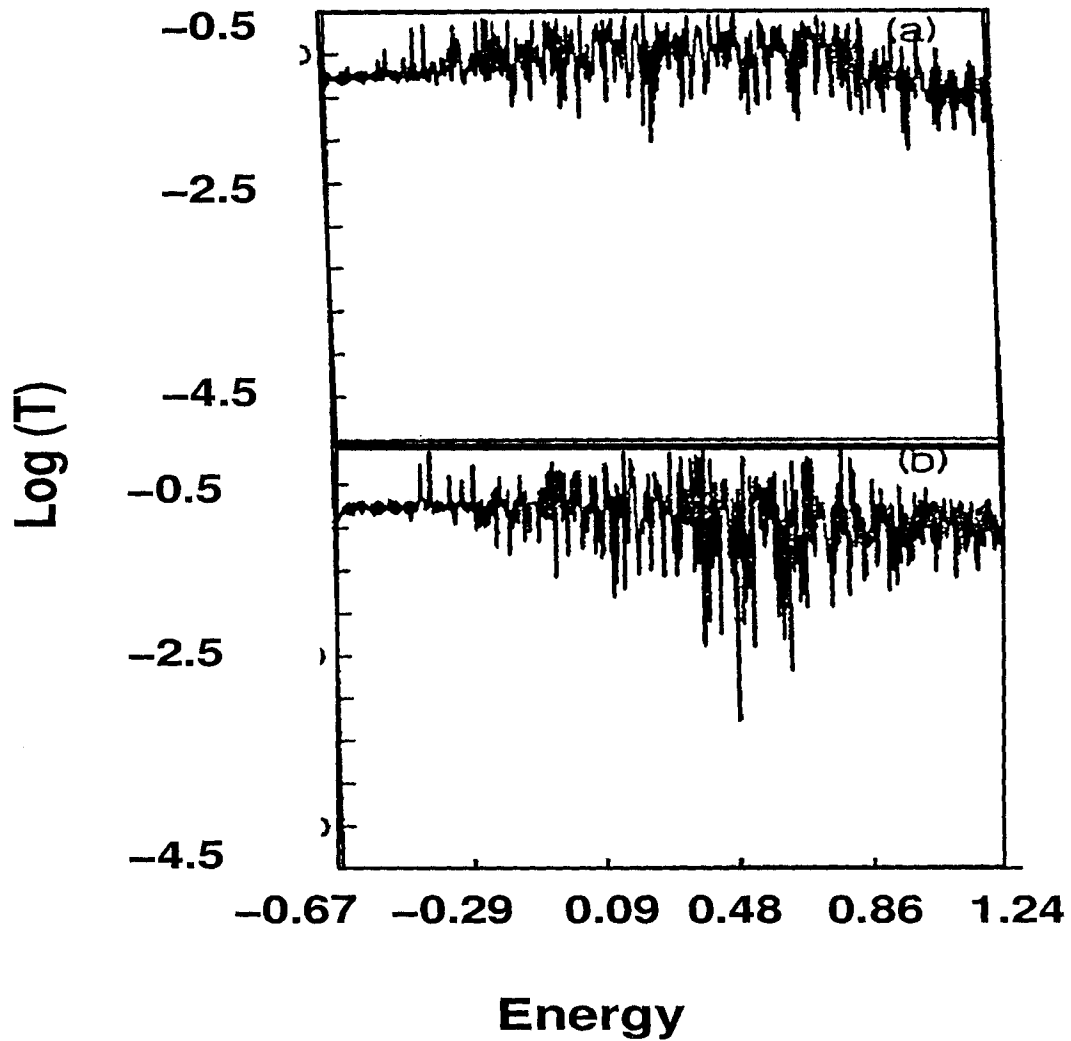


Figure 2.5: (a) Logarithm of Transmittance *vs* Energy for $\epsilon_A=0.5$, $\epsilon_B=0.25$, $c=0.1$, $V_c=1$ in the four lead geometry with $N = 2256$ (b) same as (a) but for $\epsilon_A=0.42$, $\epsilon_B=0.30$, $c = 0.20$

Next we go over to a situation where the inter-chain coupling V_c becomes the same as the intra-chain coupling V . Results for $\ln T$ vs. energy E have been shown in figures 2.5 (a) and (b) for two different set of parameters. Since more dips appear in this situation ^{and T_{\max} values decrease.} electronic states seem to become more localized at many energy points as compared to previous cases where V_c is less than V . The transmittance pattern become more fluctuating as one increases V_c .

Thus, as we increase the coupling V_c shown in the figures 2.3-2.5, one can clearly observe larger fluctuations appearing in the regime of delocalized states in the previous case. As the fluctuations grow with increasing coupling V_c , one can see that localization and delocalization compete with each other at many of the energy values. These transmittance patterns in the coupled chain case have different resonant features altogether than those in a single chain of same length.

2.5 Summary and Conclusion

In these electronic transport calculations, an attempt has been made to explore the possibility of the existence of delocalized or resonance states in two coupled chains with random dimer-type short-range correlation in the on-site potential. Calculation of the transmittance for the system has been carried out numerically using the Vector recursion algorithm of Godin and Haydock for the nearest-neighbour Anderson tight-binding model. Calculation has been done for different inter-chain coupling while the hopping along the chain has been kept constant. The calculation shows a fluctuating pattern for the transmittance (for non-zero V_c) in contrast to the single-chain case, where one observes the signature of extended states without any fluctuation. Our studies show that in the weak interchain coupling limit the single dimer chain results

still hold. However, in the strong coupling limit, quantum interference leads to fluctuations in the conductance in the vicinity of the resonance. The pattern for the four-lead geometry has resonance features ($\ln T \sim 0$) over a wide range of energies, while for other lead configurations the pattern has a different signature altogether. This is reminiscent of the typicality of quantum interference effects originating from the arrangement of input and output leads attached in a particular fashion to the sample. We think that essential features of our results also remain valid where the two chains have different configurations with same chain parameters.

This calculation highlights the different signatures of typical resonance features in the electronic states in a pair of coupled chains, with different ranges of couplings and lead configurations. The analysis draws serious attention to issues such as whether inter-chain tunneling effects are really important when dealing with electronic transport properties in realistic systems with both finite and infinite chain lengths. We do hope that the model of coupled random-dimer chains may provide some insight into modeling more realistic systems where short- ranged order may be present.

Chapter 3

Characterization of transmission resonances

3.1 Introduction

Various one dimensional models of potentials which are neither completely random nor periodic have been studied, and people have claimed that extended states exist within the spectrum (all models referred in Chapter 2 and Macia and Dominguez (1996)). Among all of the models studied so far, the random-dimer model (RDM), introduced in the previous chapter (Wu and Phillips (1991), Phillips and Wu (1991), Dunlap *et al* (1990), Datta *et al* (1993), Datta *et al* (1993), Gangopadhyay and Sen (1992), Basu and Thakur (1995)) has gained importance since Wu and Phillips claimed that it has a direct connection with the electronic transport of the polyaniline system. It has been shown by many authors that the random-dimer-type impurity potential yields electronic states which are drastically different from those of the random potential (i.e. without any short-range or long-range correlation) where one expects all states to be exponentially localized, except a few exponentially nar-

¹This chapter is partly based on the published paper : Thakur and Mitra, *J. Phys.: Condens. Matter* **9** 8985 (1997)

row resonances. Here we will recall some important physical aspects related to the RDM and we will confine our discussion to the context of the Anderson tight-binding model. In the case of the RDM, Anderson's tight-binding Hamiltonian is taken in such a manner that the impurity on-site energy ϵ_a occurs only in pairs embedded randomly in the host sample having on-site energy ϵ_b . Dunlop, Wu and Phillips (1991) showed that the reflection coefficient of a system containing a single dimer vanishes when the incoming electron energy becomes the same as the dimer on-site energy, provided that $|\epsilon_a - \epsilon_b| \leq 2V$, where V is the nearest-neighbour hopping integral. They also claimed that \sqrt{N} states get extended over the whole sample if it contains N sites. However, Gangopadhyay and Sen (1992) claimed that for a system containing randomly placed dimers there are $N^{1/3}$ ballistic states. Datta *et al* (1993) claimed that the number of non-scattered states depends also on the dimer on-site energy and its concentration in the chain. In a later publication, Datta *et al* (1993) studied the nature of states in a RDM through bandwidth scaling analysis. They claimed that the scaling behaviour of the bandwidths shows that the system contains extended states in the vicinity of the dimer on-site energy.

It has been established analytically that the electronic transmittance or wavefunction corresponding to the dimer on-site energy will always satisfy the non-scattering condition, and hence the transmittance will be unity even for an infinitely large system. However, the nature of the electronic transmittance for other energy values has not been analytically established yet. There is still some controversy regarding the nature of the electron delocalization or metallic behaviour around the dimer on-site energy (Datta *et al* (1993), Gangopadhyay and Sen (1992)). A detailed numerical study of the transmittance resonances at different energies may be

one possibility for resolving the controversy. Also, we think that in order to understand the electronic transport in the RDM more directly, one should attempt to construct a formalism of multifractal analysis for the normalized electronic transmittance to investigate different states around the dimer on-site energy. It is to be noted that the direct connection between the results that one obtains from the bandwidth scaling analysis for the RDM and the transmittance resonances for the RDM is not obvious. It should also be noted that the multifractal scaling analysis for the normalized transmittance has been previously successfully performed to make the distinction between critical, extended and localized states in the generalized Aubry model (Thakur *et al* (1992)) and also to analyze the nature of Azbel resonances in 1-D random potentials (Azbel and Soven (1983)).

We have carefully studied the spatial variation of the electronic transmittance through a multifractal scaling formalism to analyze the nature of the electron delocalization in the immediate vicinity of the dimer on-site energy and in a regime which is slightly away from the immediate vicinity. In an earlier work, a distinction between the states at the centre of the plateau region and stochastic resonances far away from the plateau region was made through multifractal scaling analysis (Basu and Thakur (1995)). In contrast, here, a distinction is made between different states in the immediate vicinity of the dimer on-site energy and states slightly away from this region. Also, we use the tight-binding Hamiltonian instead of the arrays of delta-function potential models used by Thakur *et al* (1992) and Basu and Thakur (1995).

3.2 Electronic transmittance in the transfer matrix method

Here we consider, as before, the Anderson tight-binding Hamiltonian (\hat{H}) with nearest-neighbour overlaps :

$$\hat{H} = \sum_i \epsilon_i |i\rangle \langle i| + \sum_{i,j} V_{ij} |i\rangle \langle j|$$

For the stationary-state solution of the above Hamiltonian corresponding to the energy eigenvalue E , we can write

$$|\Psi(E)\rangle = \sum_i C_i |i\rangle$$

Substituting this in the Schrödinger equation we get,

$$(E - \epsilon_i)C_i = V_{i,i+1}C_{i+1} + V_{i,i-1}C_{i-1} \quad (3.1)$$

Now we consider a situation where the first and the $(N + 1)$ th sites of a RDM chain are attached to two perfectly conducting semi-infinite leads. Following Thakur *et al* (1992) the site amplitudes in the leads are

$$C_i = \begin{cases} A_k^+ e^{ikn} + A_k^- e^{-ikn} & \text{for } i \geq (N + 1) \\ B_k^+ e^{ikn} + B_k^- e^{-ikn} & \text{for } i \leq 1. \end{cases} \quad (3.2)$$

Then, using the standard transfer matrix procedure, one can connect the incoming and outgoing solutions as follows:

$$\begin{bmatrix} A_k^- \\ A_k^+ \end{bmatrix} = T(k_j N) \begin{bmatrix} B_k^- \\ B_k^+ \end{bmatrix} \quad (3.3)$$

where

$$T(k; N) = \begin{pmatrix} e^{ik(N+1)} & 0 \\ 0 & e^{-ik(N+1)} \end{pmatrix} \mathbf{S}^{-1} \left[\prod_{i=1}^{N+1} \mathbf{P}_i \right] \mathbf{S}$$

$$\mathbf{S} = \begin{pmatrix} e^{-ik} & e^{ik} \\ 1 & 1 \end{pmatrix}$$

and

$$\mathbf{P}_i = \begin{bmatrix} (E - \epsilon_i)/V & -1 \\ 1 & 0 \end{bmatrix} \quad (3.4)$$

Now, to calculate the transmittance, we take A_k^- to be zero. The reflectance can be obtained from

$$r(E, N) = \left| \frac{B_k^-}{B_k^+} \right|^2 \quad (3.5)$$

and the transmittance $t(E, N)$ from the relation $t(E, N) = 1 - r(E, N)$.

3.3 Multifractal Scaling

The formalism of Multifractal Analysis has been used fruitfully to analyze the spatial form and to capture the degree of fluctuations at different length scales of the wavefunctions in systems where there is either a randomness or a inhomogeneity in the underlying potential.

In general, Multifractal Analysis is used to characterize a geometrical object or a probability distribution taken as a suitable measure and has wide application in different fields of theoretical physics.

First of all, we give an introduction to this formalism (see Hilborn (1994)).

What has come as a surprise to most scientists and mathematicians is that geometric objects with dimensionalities that are not integers play a fundamental role in different physical systems like the wavefunctions in a translationally non-invariant potential or a growing surface film. These geometric objects have been named fractals Mandelbrot (1982) because their dimensionality is not integer. Unfortunately, there are many apparently different definitions of dimensionality in the literature. We restrict our discussion to a measure called the *box counting dimension* (often called the capacity dimension) because a set of boxes is used in the calculation. The box-counting dimension D_b of a geometric object is determined by constructing boxes of side length R to cover the space occupied by the geometric object under consideration. For 1-D sets, the boxes are line segments of length R and in 2-D, they would be squares of length R . We now count the number of boxes $N(R)$ needed to contain all the points of the geometric object. The box-counting dimension D_b is defined to be the number that satisfies

$$N(R) = \lim_{R \rightarrow 0} K R^{-D_b}$$

where K is a proportionality constant. In practice, we find D_b by taking the logarithm.

$$D_b = \lim_{R \rightarrow 0} \left[-\frac{\log N(R)}{\log R} + \frac{\log K}{\log R} \right]$$

As $R \rightarrow 0$, the last term goes to zero. If we consider a number of isolated points as our geometric object, then D_b equals to 0, and for a line segment, D_b equals to 1. It is illuminating to consider the case of the Cantor set to have a feel for a fractal object. A Cantor set is constructed in the following way : a line segment is taken

and the middle third of it is deleted. We delete the middle third of each of the remaining line segments. If we repeat this process M times and let $M \rightarrow \infty$, then what is left is the cantor set. It can be shown that D_b for this set is 0.63. So the cantor set is more than isolated points but less than a line segment.

The box counting dimension is an average over the whole geometric object. Now two geometric objects or two statistical distributions may have the same value for an average value but the local contributions from different parts of the two objects may vary considerably. So it is necessary to calculate the so-called moments of the distribution to fully capture the statistical distribution. This motivates to introduce the generalized box counting dimension D_q .

Probably the most extensive application of Multifractal Formalism has been in the field of non-linear dynamics and it is easy to get a feel for the Multifractal formalism if we consider the attractor of a dissipative classical dynamical system as our geometric object to be characterized. An attractor is that set of points to which trajectories approach as the ~~time~~ $t \rightarrow \infty$. Suppose we have N trajectory points on an attractor. As before, we divide the attractor region of state space into cells of size R labelled $i = 1, 2, 3 \dots N(R)$. In general $N \neq N(R)$ and also the number of cells depends on R . If N_i be the number of trajectory points in the i th cell then we define the probability p_i to be the relative number of trajectory points r in the i th cell $p_i = \frac{N_i}{N}$. The generalized (Box-counting) dimension D_q is then defined by

$$D_q = \lim_{R \rightarrow 0} \left(\frac{1}{q-1} \right) \frac{\log \sum_{i=1}^{N(R)} p_i^q}{\log R}$$

Here q can be any real number. Above, the case when q equals to 1 has to be

taken for $q \rightarrow 1$. Here it is possible to characterize the fluctuations upto a minimum length scale R . As $q \rightarrow \infty$, the largest probability value, say p_{\max} will dominate the sum in the above equations.

$$D_{\infty} = \lim_{R \rightarrow 0} \frac{\log p_{\max}}{\log R}$$

Again, when $q \rightarrow -\infty$, the smallest probability value p_{\min} will dominate the sum. Hence we find that D_{∞} is associated with the most densely occupied region of the attractor while $D_{-\infty}$ is associated with the most rarefied region of the attractor. We can visualize this object as a collection of overlapping fractal objects each with its own fractal dimension. Such an object is called a Multifractal. It is clear that in the case of translationally non-invariant potential, the wavefunctions may have the same power-law or exponential form but still may be very different in their appearance. This is why the multifractal description seems to be an appropriate description for an electronic state.

Now a natural question to ask is how many regions have a particular value on range of values of the fractal dimension. A very powerful scheme has been developed to answer that question. That scheme provides a distribution function, usually denoted by $f(\alpha)$ and called the ‘singularity spectrum’ which gives the distribution of the ‘scaling exponents’ (also known as Lipschitz-Hölder exponent) which in turn characterizes the singularity strength of the fractal. So here we assume that $p_i(R_i)$ satisfies a scaling relation

$$p_i(R_i) = K R_i^{-\alpha_i}$$

where K is same (unimportant) proportionality constant and R_i is the size of the

i th cell. The crucial assumption is that we expect the number of cells with α in the range α to $\alpha + d\alpha$ to scale with the size of the cells with a characteristic exponent, which we call $f(\alpha)$. i.e. $n(\alpha) \sim R^{f(\alpha)}$. The relation $f(\alpha)$ completely characterizes the multifractal.

The connection between $f(\alpha)$ and D_q is most easily established by looking at the probability sum, known as the partition function $Z_q(R) = \sum_{i=1}^{N(R)} p_i^q$.

In order to make the connection to $f(\alpha)$, we write the probabilities in terms of α and then integrate over the distribution of α values to get the partition function

$$Z_q(R) = C \int d\alpha R^{f(\alpha)-q\alpha}$$

where C is an unimportant proportionality constant. The first factor in the integrand tells how many cells have scaling index α while the second factor is the q th power of the probability associated with index α . One can now show after some mathematical manipulations that

$$\begin{aligned} (q-1)D_q &= -q\alpha + f(\alpha) \\ \alpha(q) &= -\frac{d}{dq}[(q-1)D_q] \\ f(\alpha) &= -q\frac{d}{dq}[(q-1)D_q] + (q-1)D_q \end{aligned} \quad (3.6)$$

To summarize, we see that once we have found D_q as a function of q , we can compute $f(\alpha)$ and α . This change from the variables q and D_q to α and $f(\alpha)$ is an example of an Legendre Transformation commonly used in the formalism of thermodynamics. Although $f(\alpha)$ and α are based on the D_q 's the necessity of going

through the extra computational trouble to get α and $f(\alpha)$ arises due to relatively simple interpretation of various aspects of the $f(\alpha)$ curve and due to the fact that this curve displays in a straightforward manner some expected universal features.

In our studies, we define the measure p_i in terms of the normalized transmittance as

$$p_i = \frac{T_i(E)}{\sum_{i=1}^N T_i(E)} \quad (3.7)$$

where T_i is the transmittance from one end of the chain upto the i th segment when the length of the chain is divided into N equal segments such that transmittance for a given size is obtained by always increasing the previous size by adding one segment.

We shall use a formalism due to Chhabra and Jensen (1989) where one need not calculate the generalized D_q to get the $f(\alpha)$ singularity spectrum. This algorithm has been used to carry out multifractal analysis for characterization of states in the Aubry model and a continuous correlated disorder model (Basu and Thakur (1995)).

According to Chhabra and Jensen (1989) if one defines the Q -th moment of the probability measure by the following expression

$$\mu_i(Q; N) = \frac{p_i^Q}{\sum_{i=1}^N p_i^Q} \quad (3.8)$$

then a complete characterization of the fractal singularities can be made in terms of this function and one can derive the spectrum of the fractal singularities defined by $\{\alpha, f(\alpha)\}$ as :

$$\begin{aligned}
f(\alpha) &= \lim_{N \rightarrow \infty} \left[-\frac{1}{\log N} \sum_{i=1}^N \mu_i(Q; N) \log \mu_i(Q; N) \right] \\
\alpha &= \lim_{N \rightarrow \infty} \left[-\frac{1}{\log N} \sum_{i=1}^N \mu_i(Q; N) \log p_i \right]
\end{aligned} \tag{3.9}$$

From the definition of transmittance $p_i \geq 0$ and $\sum_{i=1}^N p_i = 1$. The singularity strength α is found from the scaling behaviour $p_i \sim N^{-\alpha}$ and the corresponding 'singularity spectrum' $f(\alpha)$ is given by

$$N_\alpha \sim N^{f(\alpha)}$$

where N_α be the number of boxes (segments) which cover the measure having exponents between α and $\alpha+d\alpha$. The Multifractal analysis of the measure defined in (3.7) has been previously done to characterize successfully the states in random potential Basu *et al* (1991) and also the critical states in generalized Aubry Models(Thakur *et al* (1992)).

It follows that for an extended state, $f(\alpha)$ vs α curve should converge inwards and asymptotically it converges into the point $(\alpha = 1, f(\alpha) = 1)$. On the other hand for a localized state, α minimum should get smaller and smaller with the increase of system size corresponding to a large probability for getting the electron within the localization length (ideally =1, so that one has $f(\alpha = 0) = 0$) Also, α_{\max} should become larger and larger, implying that the other sites have probability 0, so $\alpha = \infty$ and $f(\alpha = \infty) = 1$. For the states which are not extended and not exponentially localized one should get a smooth $f(\alpha)$ curve asymptotically having a rich singularity spectrum.

3.4 Results and Discussion

In our numerical work, we have considered the hopping parameter to be unity in the lead as well as in the sample and all other energy parameters have been considered in units of the hopping term throughout the calculations. First of all, we numerically compute the electronic transmittance for a chain having the dimer on-site energy $\epsilon_A = 0.45$ units and the host on-site energy $\epsilon_B = 0.145$ units, the concentration c of the dimer impurity being 0.10 for the two different system sizes. The transmittance $T(E)$ versus energy (E) plot for $N = 2 \times 10^4$ sites is shown as the upper curve in figure 3.1. The lower curve shows the transmittance $T(E)$ versus energy E plot for a large size - $N = 2 \times 10^5$ sites. Here, due to the increase of the system size, we see that the energy region around the dimer on-site energy over which the transmittance $T(E)$ is nearly flat, forming a plateau, and that region shrinks.

We have analyzed the spatial characteristics of the transmittance in the vicinity of the dimer on-site energy and have gradually crossed these nearby energies to establish whether the behaviour of the spatial form of the transmittance changes from the behaviour in the immediate vicinity. We have shown this by plotting the transmittance $T(E)$ for different lengths for these energy values in figure 3.2. The top curve shows the transmittance versus length plot for the transmission resonance at $E = 0.45228$ units. The middle curve is the same plot but for the resonance state at $E = 0.47216$ units, i.e. the energy value is chosen slightly away from the immediate vicinity, where one can see some changes, and a new pattern starts showing up. The lowest curve shows the variation of the transmittance $T(E)$ with length (N) for $E = 0.47192$ units. It is to be noted that the value of the transmittance for $E = 0.47192$

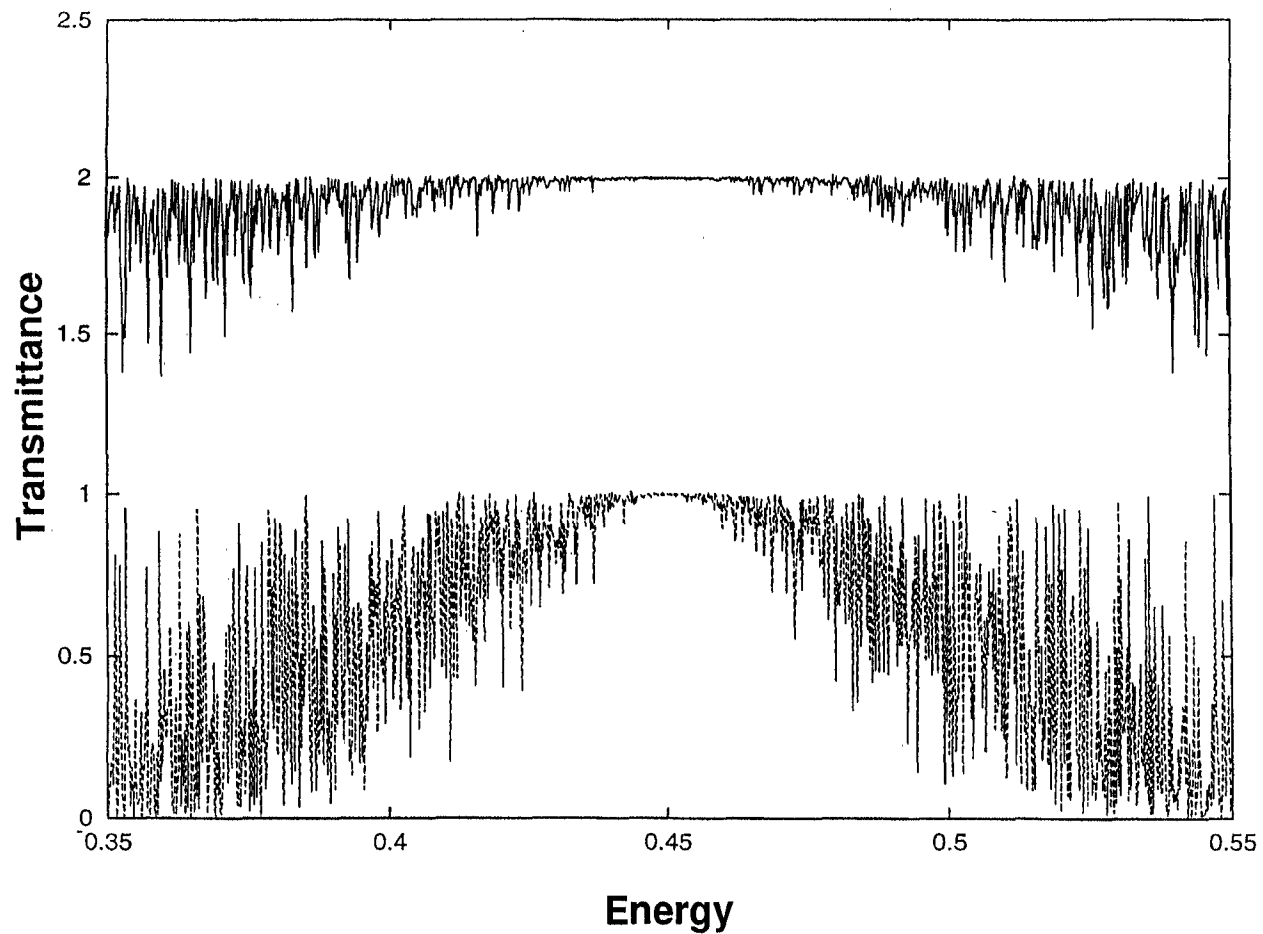


Figure 3.1: Transmittance *vs* energy for $\epsilon_A=0.45$, $\epsilon_B=0.145$, $c=0.1$ and (lower) $N=2 \times 10^5$ (upper) $N=2 \times 10^3$, upper graph shifted vertically by one unit

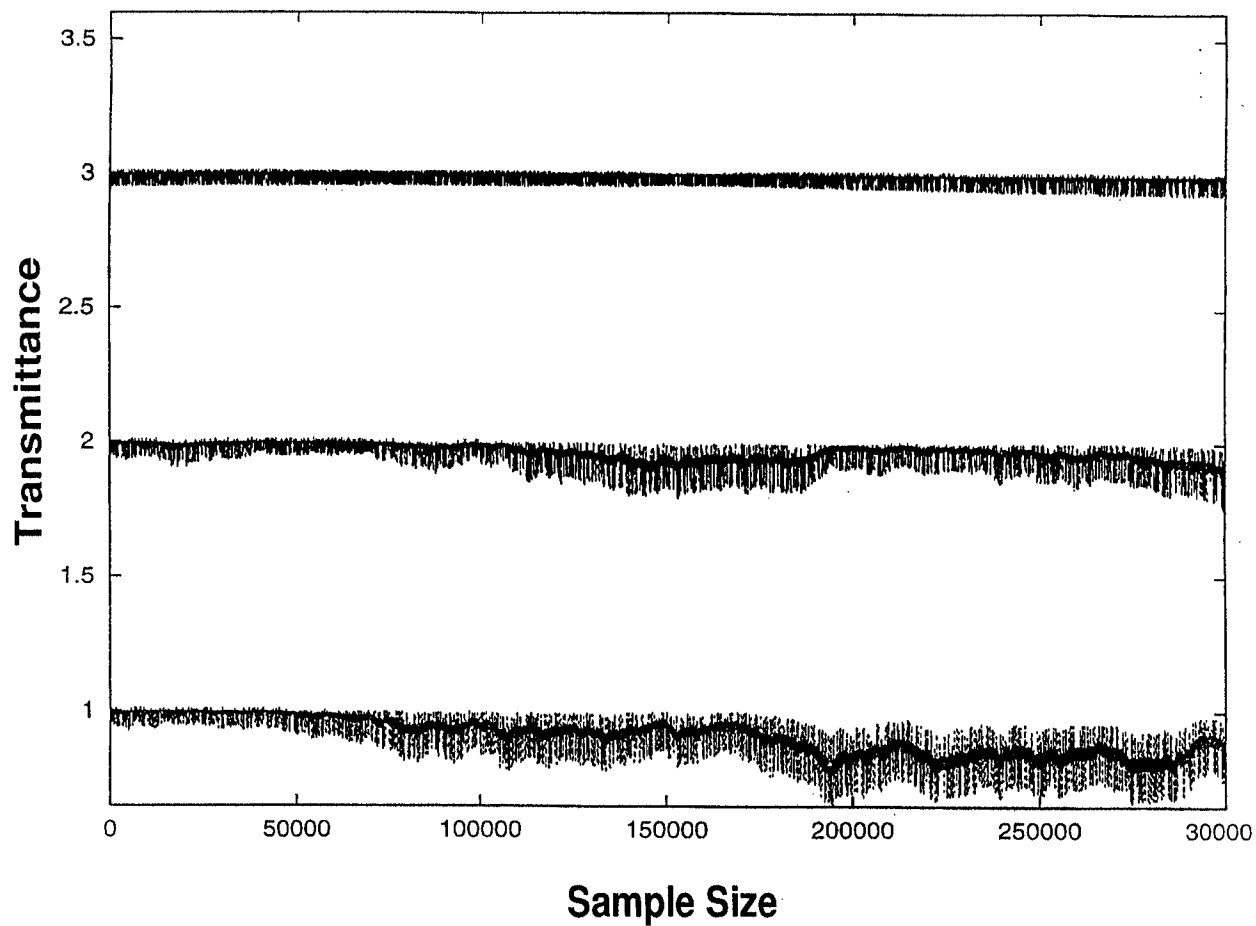


Figure 3.2: Transmittance vs sample size for (top) $E=0.45228$ and (middle) $E=0.47216$ (bottom) $E=0.471920$ for the same parameters as figure 3.1, upper graphs shifted vertically by one unit

units is lower than that for the energy value $E = 0.47216$ units. One can think of this energy region as being a physically different region, where a new pattern in the transmittance versus length plot emerges, as compared to the region immediately around the dimer on-site energy. We have performed a multifractal scaling analysis *i.e.* produced $(\alpha, f(\alpha))$ -plots for these states, as described below.

In figure 3.3(a) the $f(\alpha)$ versus α plot is shown for $E = 0.45228$ units for three different system sizes : $N = 5 \times 10^4, 10^5$ and 2×10^5 sites. One can notice that with the increase of the system size, the $f(\alpha)$ versus α curves contract systematically. This is a clear signature of a Bloch-like extended state.

In figure 3.3(b), we have shown an $f(\alpha)$ versus α curve for $E = 0.47216$ units and for $N = 1.5 \times 10^5, 2 \times 10^5$, and 3×10^5 sites, where we see that both the α_{\min} and α_{\max} values are now increased in magnitude, but it does not shown any definite trend of either a contraction or a systematic increase with system size. However, the α_{\min} values do not change significantly. Here clearly the $\alpha, f(\alpha)$ spectrum signifies the deviation from both the typical Bloch-like extended character and from the exponentially localized nature. In this sense, this is a region that is physically different from the immediate vicinity, where the Bloch-like extended character is observed.

In figure 3.3(c), we have shown the $f(\alpha)$ plotted against α for $E = 0.47192$ units and for $N = 1.0 \times 10^5, 1.5 \times 10^5$, and 2.5×10^5 sites, where with the increase of the system size, a tendency towards localization is observed. Here the exponents α and $f(\alpha)$ do not deviate much from unity, and this is a manifestation of a slow electronic localization in the neighbourhood of the actual resonance.

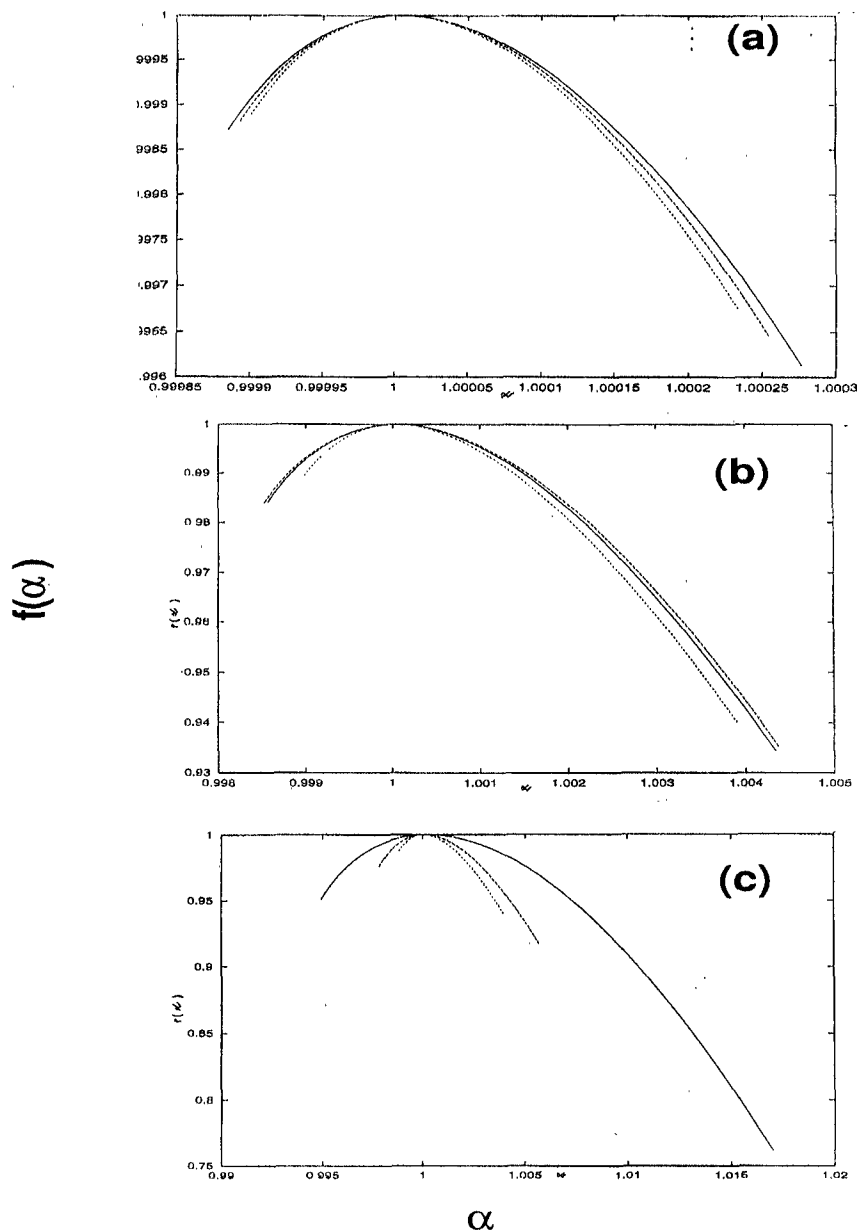


Figure 3.3: $f(\alpha)$ vs α for the same set of parameters as in figure 3.1 and (a) $E=0.45228$ and sizes (bold) $N = 5 \times 10^4$ (dashed) $N = 1 \times 10^5$ (dotted) $N = 2 \times 10^5$ (b) $E=0.47216$ and sizes (bold) $N = 3 \times 10^5$ (dashed) $N = 2 \times 10^5$ (dotted) $N = 1.5 \times 10^5$ (c) $E=0.471920$ and sizes (bold) $N = 2.5 \times 10^5$ (dashed) $N = 1.5 \times 10^5$ (dotted) $N = 1 \times 10^5$

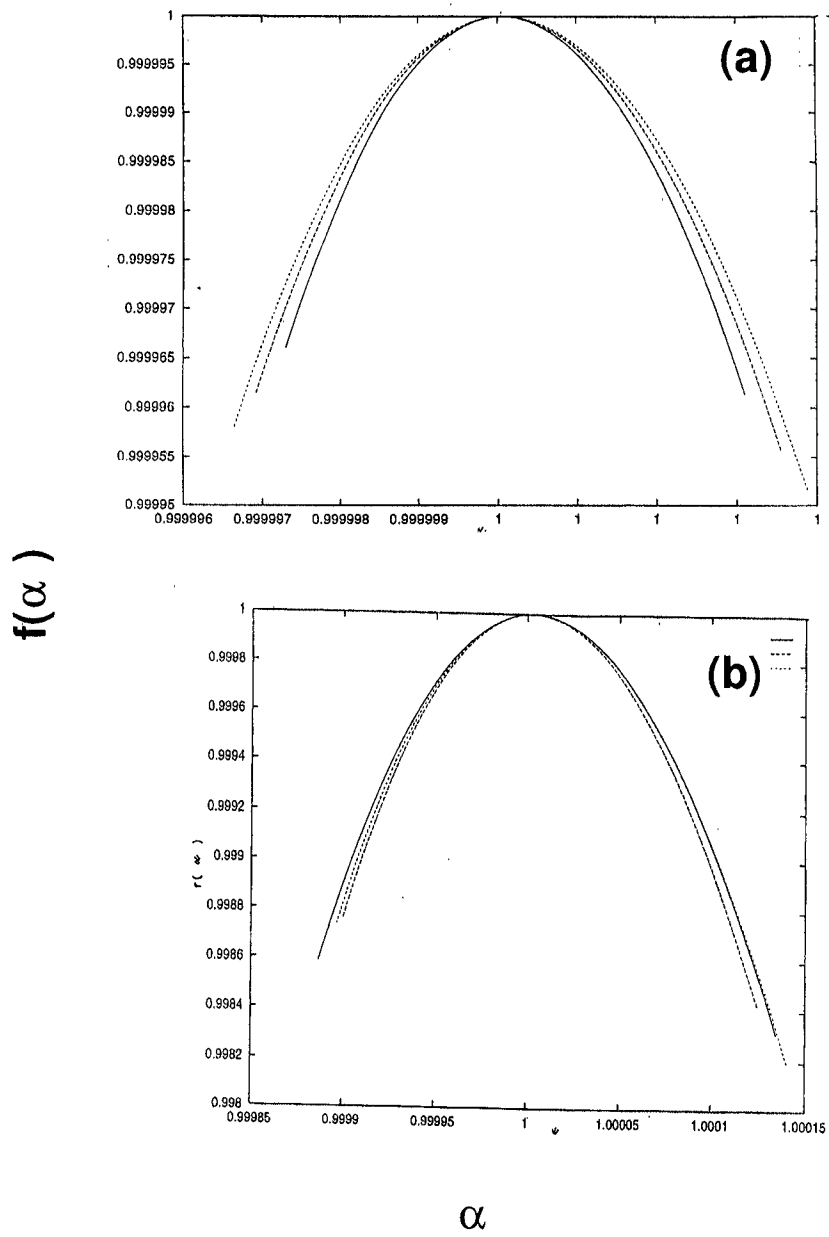


Figure 3.4: $f(\alpha)$ vs α for $\epsilon_A=0.15$, $\epsilon_B=0.045$, $c=0.15$ (a) $E=0.15246$ and sizes (bold) 2.5×10^5 (dashed) 1×10^5 (dotted) 5×10^4 (b) $E=0.18992$ and sizes (bold) 3×10^5 (dashed) 1×10^5 (dotted) 5×10^4 .

Next, we consider the case where the impurity site energy $\epsilon_A = 0.15$ units, and $\epsilon_B = 0.045$ units, and the impurity concentration $c = 0.15$. In figure 3.4 (a), the $f(\alpha)$ versus α plot has been shown for the energy value $E = 0.15240$ units and for three different system sizes, i.e. $N = 5 \times 10^4, 10^5$, and 2.5×10^5 sites. One can clearly see that with the increase of the system size the curves systematically contract signifying a Bloch-like extended state.

Now, if one carefully analyses another set of $f(\alpha)$ versus α curves as shown in figure 3.4(b) for the resonance state at $E = 0.18992$ units for three system sizes, $N = 5 \times 10^4, 10^5$, and 3×10^5 sites, one can notice that the curves do not systematically contract, but on the other hand the α_{\max} and α_{\min} values show small oscillations. In this situation, the values of α and $f(\alpha)$ are not very different from unity, and the deviation from the Bloch-like extended character is much less as compared to the resonance state shown in figure 3.3(b). This is due to the choice of a smaller difference of ϵ_A and ϵ_B i.e. the on-site energies of the dimer and the host, so the values of transmittance are always relatively high, i.e. closer to unity. Note that both these resonances are characterized by finite energy widths as compared to the exponentially narrow Azbel resonances.

3.5 Summary and Conclusions

Our numerical study of the electronic transmittance corresponding to the transmission resonances both in the vicinity of the dimer on-site energy and slightly away from it brings into focus important physical aspects which have not been properly investigated before. The transmission resonances for energies very close to the dimer on-site energy exhibit extended character similar to that of Bloch-type wavefunctions.

There are also other resonances of finite width away from this region for which the spatial variation of the transmittance exhibits a strongly fluctuating pattern which persists upto a very large system size.

In this region there are some energy points where the behaviour of transmittance is like that of states undergoing slow localization. This is shown in figure 3.3(c).

Although Gangopadhyay and Sen (1992) observed the existence of these two regions, they did not attempt any rigorous numerical analysis to distinguish the two. Also, in contrast to their speculation that the nearby states will behave like critical states under multifractal analysis, we find a Bloch-like extended character for these states by the same analysis. We claim that the spatial behaviour of the electronic transmittance for energies slightly away from the immediate vicinity of the dimer on-site energies is different from that of Bloch-like extended states and exponentially localized states and also from that of exponentially narrow Azbel resonances.

According to Wu *et al* (1992), any physical system such as conducting polymers or semiconductor heterostructures that can be described by the RDM should exhibit transmission resonances and a drastic enhancement in its conductivity when the Fermi level coincides with the position of the resonance states. We believe also that the transmission resonances where the transmittance shows a behaviour different both from Bloch-like extended states and from exponentially localized wavefunction may cause enhancement of the conductivity in such systems.

Chapter 4

Electronic Transmittance and Localization in quasi-1d systems of coupled identical n-mer chains¹

4.1 Introduction.

In one dimensional disordered systems, which have no short-ranged correlation between the random potentials, almost all electronic eigenstates are localized. The single parameter scaling arguments supports this statement. It came as a mild surprise that with short-ranged correlations among the random potentials, a regime of electronic states do get extended (Basu and Thakur (1995), Datta *et al* (1993), Soukoulis *et al* (1994), Giri *et al* (1993), Sil *et al* (1993), Chakraborti *et al* (1995), Heinrichs (1995) and also those in the footnote in Chapter 2). Disagreement with the scaling theory may be attributed to the introduction of another intrinsic scale in the Hamiltonian, thus making the single parameter scaling theory inadequate. Of all the models studied in this context, the Random Dimer model (RDM) has a special feature, as Wu and Phillips have shown, that the Hamiltonian of some conducting

¹This chapter is partly based on the published paper : Mitra and Thakur, *Int. J. Mod. Phys. B* **12** 1773 (1998)

aniline derivatives can be related to this model. In RDM model, the Anderson's tight-binding Hamiltonian is taken in such a manner that the impurity with site energy e_A occurs only in pairs embedded in a host sample having site energy e_B . The nearest neighbour hopping parameter is kept at a constant V . According to Wu and Phillips, the enhanced conductivity of these aniline derivatives is due to these extended states. Random n -mer models are generalizations of the above model. In this model, chains of n identical atoms are randomly embedded in the host lattice.

The Hamiltonian is given by,

$$\mathbf{H} = \sum_i e_i |i\rangle\langle i| + \sum_i \sum_{j \neq i} V_{ij} (|i\rangle\langle j| + |j\rangle\langle i|) \quad (4.1)$$

We wish to solve the Schrödinger equation :

$$\mathbf{H} |\Phi\rangle = E |\Phi\rangle \quad (4.2)$$

The wavefunction can be expanded in the tight-binding basis :

$$|\Phi\rangle = \sum_i \phi_i |i\rangle$$

ϕ_i is the projection of the wavefunction on the i -th position. Rearranging terms,

$$\begin{bmatrix} \Phi_{N+1} \\ \Phi_N \end{bmatrix} = \mathbf{M}(N) \begin{bmatrix} \Phi_N \\ \Phi_{N-1} \end{bmatrix}$$

where,

$$\mathbf{M}(N) = \begin{bmatrix} (E - e_N)/V & -1 \\ 1 & 0 \end{bmatrix} \quad (4.3)$$

Here $V_{ij} = V$ if i, j are nearest neighbours and 0 otherwise. It has been shown (Sil *et al* (1993), Chen and Xiong (1993)) that for a n -mer, if $\prod_n \mathbf{M}(n) = \mathbf{I}$, then there are $(n - 1)$ extended states provided the energy E lies within the band of the host and the corresponding energy eigenvalues are given by the relation :

$$E_\ell = e_A + 2V \cos\left(\frac{\pi\ell}{n}\right)$$

where $\ell = 1, 2 \dots (n - 1)$.

The metallic behaviour in electronic transport in conducting polymeric systems have been discussed in several earlier works in many contexts (Ducker *et al* (1992)). Wu and Phillips (1991) have pointed out that in order to describe electronic transport in polyaniline, it is necessary to consider two dimensional aspects if the transverse hopping distance between two strands is comparable to the sample length. Recently Progodin and Efetov (1993) have argued that the metallic state can exist in a network of randomly coupled metallic fibrils.

In an earlier chapter we have studied the effect of interchain coupling for two coupled RDM chains. Here we shall study the effect of finite interchain coupling in quasi $1-d$ systems consisting of identical random n -mer chains. Such models may be important in understanding the conductance pattern of some conducting polymers. In such a random n -mer system, there will be conduction if the Fermi energy lies within one of the resonance regions on the spectrum.

The results of these studies may be verified experimentally. These studies may be also important for designing new quantum devices based on the possibility of merger of several resonances (Bellani *et al* (1999), Giri *et al* (1993)).

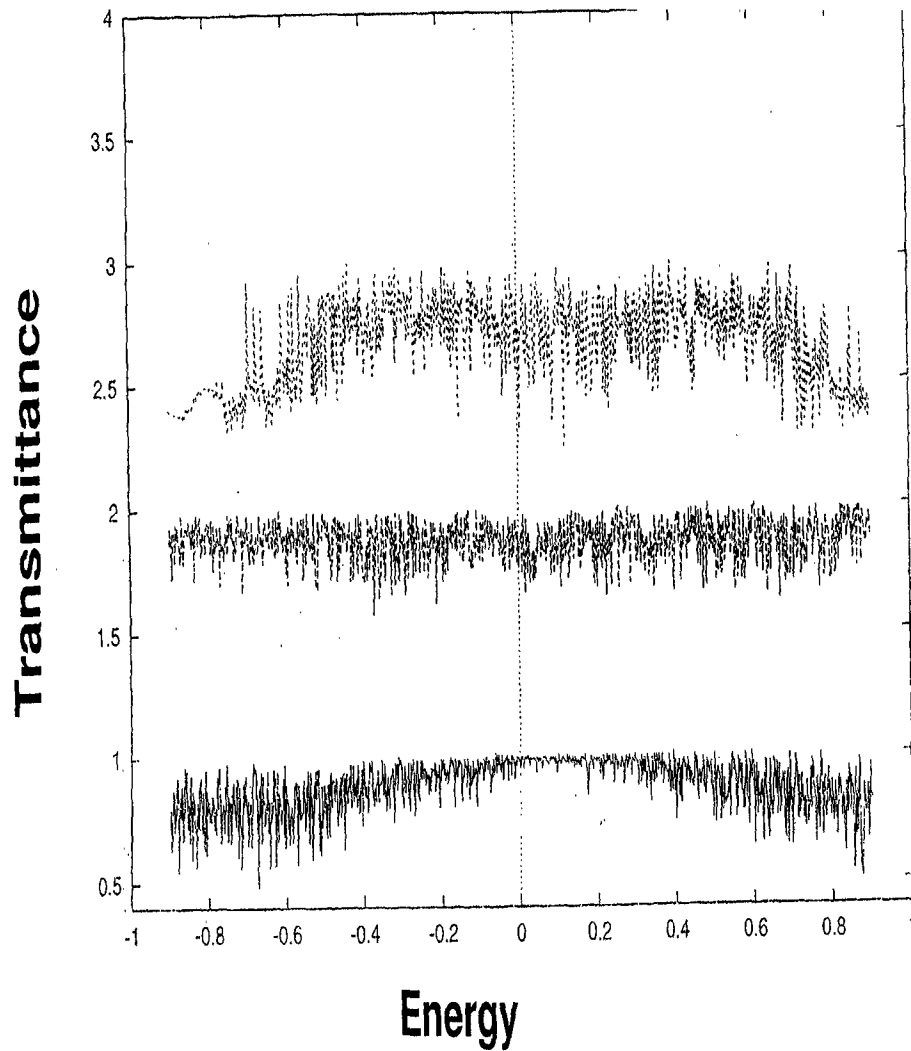


Figure 4.1: Transmittance *vs* Energy for a 4-mer in 2 chains with $\epsilon_B=0.01$, $\epsilon_A = 0.11$, $c=0.15$, $N=6000$ and (solid) $V_c=0.15$, (dashed) $V_c=0.45$ (dotted, top) $V_c=1.0$.
 (upper graphs shifted vertically by one unit)

4.2 Results and discussions

In this chapter we present a detailed numerical study of transmittance for two coupled random 4-mer chains, four coupled random 4-mer chains and two coupled 3-mer chains. This is in order to examine the effect both of coupling to many chains and changing size of the impurity n -mer. The reason behind choosing different sized n -mers is to study whether different regimes of extended states may merge together to form a wide metallic region.

We shall use the Vector Recursion technique of Godin and Haydock (1988) for the calculation of transmittance and reflectance. The algorithm has been described in great detail in Chapter 2.

In Figure 4.1 we plot the transmittance $T(E)$ versus the energy E for two coupled chains of 4-mers. The size of the chains were 6000 units, all chains were random 4-mers. As the interchain coupling is raised from 0.15 to 1.0 unit, the inherent fluctuations also increase.

In Figure 4.2 we have shown transmittance versus energy for four coupled 4-mer chains of two different sizes. When the size is increased from 2000 to 6000 units, leaving the interchain coupling a constant, the overall pattern contracts and the number of dips in the pattern increases. In Figure 4.3 we have changed the interchain coupling for two coupled 3-mer chain from 0.15 to 1.0, while keeping the intrachain coupling to be a constant 1. In all cases we observe an overall increase in fluctuation as the coupling term increases. In fact, due to finite interchain coupling, the frequency and amplitude of transmittance fluctuations increase with the increase of both system size as well as interchain coupling. The indication is that finite

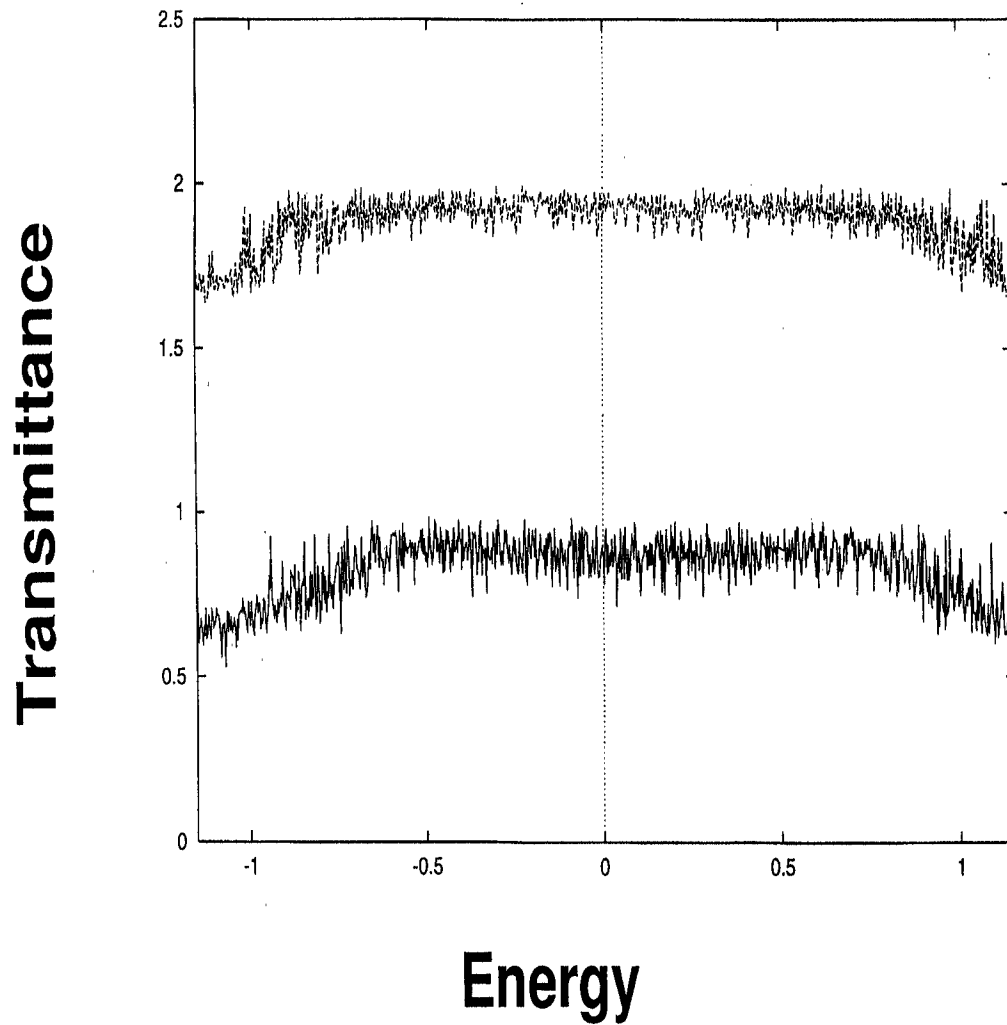


Figure 4.2: Transmittance vs Energy for a 4-mer in L_1 chains with $\epsilon_A=0.11$, $\epsilon_B = 0.01$, $c=0.15$, $V_c=0.5$ and (solid) $N=6000$ and (dashed,top) $N=2000$ (upper graph shifted vertically by one unit)

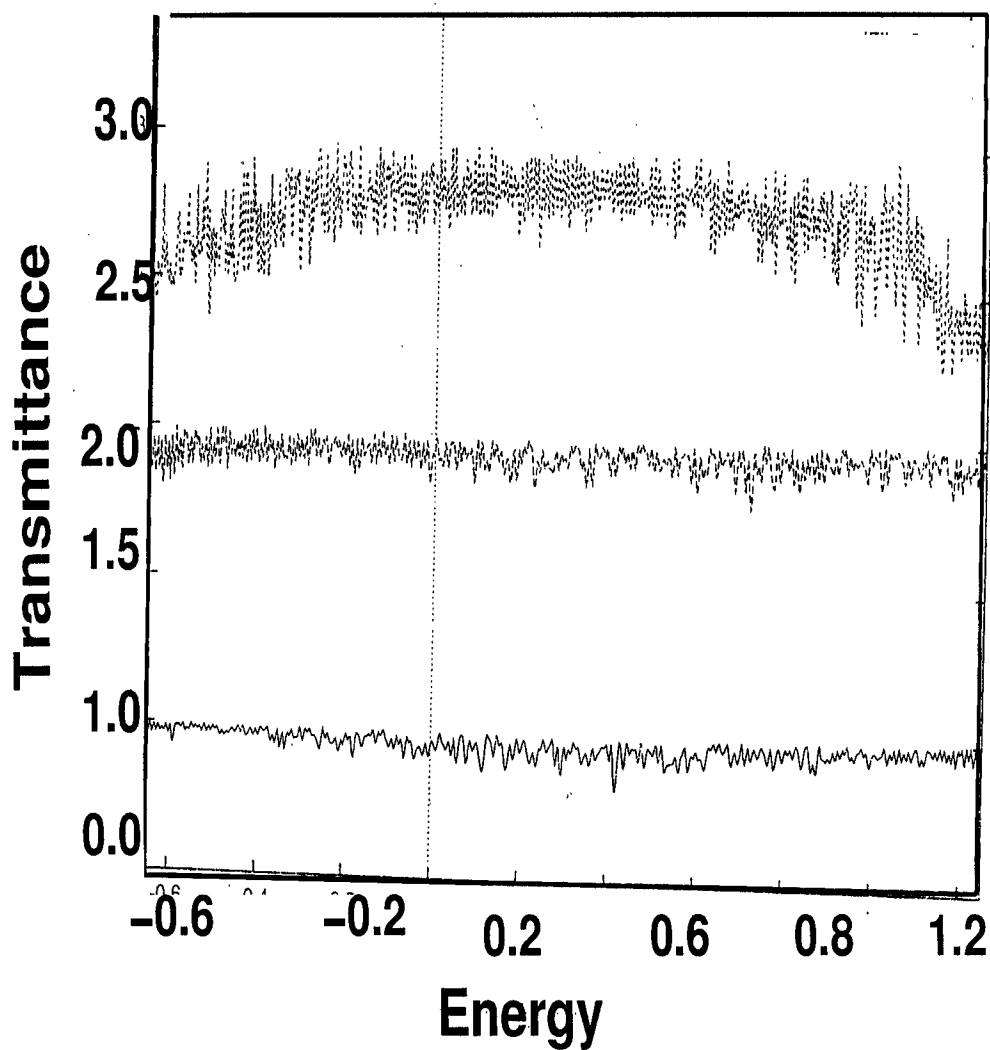


Figure 4.3: Transmittance vs Energy for a 3-mer in 2 chains with $\epsilon_A=0.35$, $\epsilon_B=0.25$, $c=0.15$, $N=1140$ and (solid) $V_c=0.15$ (dashed) $V_c=0.45$ and (dotted, top) $V_c=1.0$ (upper graphs shifted vertically by one unit)

interchain coupling has a tendency to localize the states, which were strictly extended in this 1-d situation. This phenomenon can be justified by the following argument : In the case of a $1 - d$ n -mer model, contributions to total reflection coefficient from individual impurities within a cluster cancel one another at the resonance energies. That is they interfere destructively. As a result the total reflectance becomes zero and transmittance 1 at these energy points. Now, in the case of quasi $1 - d$ random n -mer model having a finite interchain coupling, due to the contribution to the total reflection coefficient from sideways, the condition for the mutual cancelation of reflection coefficients is not achieved at those energy points where resonance is observed for the single chain random n -mer model. But if the sample size is not very large and the interchain coupling is small as compared with the intrachain coupling, then the system will show metallic behaviour and several resonances may merge together to form a wide band.

Numerical studies of transmittance of random n -mer models are important for the technological purpose of designing new quantum devices because of the possibility of merger of several resonance regions producing a broad resonance pattern.

Chapter 5

A Mode Based Formulation of the Vector Recursion Technique

5.1 Introduction

In recent times, spectacular development in lithography and layer growth techniques have taken place in the field of micro-fabrication of semiconductor devices. Due to these developments, it is now possible to confine electrons in a conductor with a lateral extent of 100 nm or less in narrow quantum wires, constrictions and quantum dots.

Owing to the small size of these structures, it is possible to reduce the defect scattering and to make the electronic motion ballistic at low temperatures. In these mesoscopic systems, the dephasing factors arising from the inelastic scattering from phonons is largely suppressed and the phase coherence length of the electrons are large compared to the size of the sample and the motion of the electrons in these high mobility mesoscopic devices is similar to the propagation of microwaves in a wave guide and the idealized sample becomes an electron wave guide where the motion of electrons is quantum mechanically determined solely by the impurity configuration and the geometry of the conductor. The possibility of fabricating

electron wave guides have opened up the path for making quantum devices which are quantum analog of well known optical or microwave devices (Al'tschuler *et al* (1991), Weisbuch and Vinter (1991), Buot (1993), Mitin *et al* (1999)) Also some important quantum phenomena like quantized conductance and Aharonov-Bohm oscillations in the magneto resistance (Singha Deo and Jayannavar (1994), Washburn and Webb (1986)) have been observed in these ballistic systems. Also the dependence of quantum observables like the conductance on the nature of the underlying classical mechanics (that is its chaotic or integrable character) has been experimentally established and much theoretical work has been done on this in relation to the quantum manifestation of classical chaos. The interplay of geometry and impurities is always important to understand the physics of electronic conductance of these systems (Sols *et al* (1989), Kawamura and Leburton (1993), Leng and Lent (1993), Singha Deo and Jayannavar (1994), Berthod *et al* (1994), Nikolic and MacKinnon (1994), Haque and Khandekar (1996)). Our aim is to suggest a method to numerically calculate the electronic transmittance of these systems. Our method is a generalization of the Vector Recursion Method suggested by Godin and Haydock (Godin and Haydock (1988)). This algorithm has been found to be numerically stable in calculating electronic transmittance in 1-D, 2-D and 3-D systems (Godin and Haydock (1988), Mitra and Thakur (1996), Saha *et al* (1994)). However in all these applications of the Vector Recursion Method, although the system was taken to be either 1-D, 2-D or 3-D; the perfectly conducting incoming and outgoing leads were independent linear channels. To study the interplay of disorder and geometry in the ballistic regime of the electronic motion, it is necessary to generalize the Vector Recursion Method to incorporate fully 3-D or 2-D, as the case may be, incoming

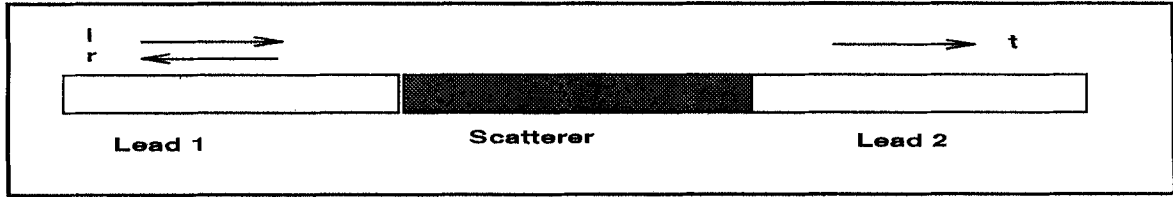


Figure 5.1: A two-dimensional scatterer with two-dimensional leads

and outgoing leads.

5.2 Formulation

5.2.1 The mode propagation picture

We shall model the scatterer by a three dimensional cubic array of sites with two semi-infinite, perfectly conducting, three dimensional leads attached to diametrically opposite faces.

A simple Hamiltonian for the motion of an electron in these perfectly conducting leads will be given by:

$$H = \sum_{\underline{n}} \sum_{\underline{m}} V_L \{ |\underline{n}\rangle \langle \underline{m}| + |\underline{m}\rangle \langle \underline{n}| \} \quad (5.1)$$

here $\{ |\underline{n}\rangle \} = \{ |n_1, n_2, n_3\rangle \}$ forms a complete, orthonormal, tight-binding like basis spanning a Hilbert space \mathcal{H} .

In case the leads were 1-D chains, the Schrödinger equation in the leads can be immediately solved to obtain Bloch-like *incoming* and *outgoing* solutions:

$$|k\rangle = \sum_n \Psi_n(k) |n\rangle$$

such that

$$\Psi_n(k) = \frac{1}{\sqrt{2\pi}} \exp(\pm ikn) \quad (5.2)$$

The Bloch label k is related to the energy of the travelling electrons through the dispersion relation: $E/2V_L = \cos k$. Non-evanescent states therefore travel through the leads in the energy window $-2V_L \leq E \leq 2V_L$.

For a full three-dimensional lead, we have to impose boundary conditions on the four finite faces of the lead. The simplest boundary conditions are periodic ones. In this case, the solution becomes:

$$|k_{\mu\nu}, \mu, \nu\rangle = \sum_{n_1} \sum_{n_2} \sum_{n_3} \Psi_{n_1, n_2, n_3}(k_{\nu\mu}, \nu, \mu) |n_1, n_2, n_3\rangle$$

such that

$$\begin{aligned} \Psi_{n_1, n_2, n_3}(k_{\nu\mu}, \nu, \mu) &= N_{\mu\nu} \exp(\pm i k_{\nu\mu} n_1) \exp\left(\frac{2\pi i \nu}{N-1} n_2\right) \exp\left(\frac{2\pi i \mu}{M-1} n_3\right) \\ &= N_{\mu\nu} \exp(\pm i k_{\nu\mu} n_1) F(\mu, \nu, n_2, n_3) \end{aligned} \quad (5.3)$$

$N_{\mu\nu}$ is the normalization factor associated with the Fourier basis in equation 5.3. The cross-section of the leads have $N \times M$ sites. The indices $\nu = 0, 1, \dots, N-1$ and $\mu = 0, 1, \dots, M-1$ label the various allowed modes that can propagate in the leads. Note that there are as many modes as there are sites in the lead cross-sections. The dispersion relation will be given by:

$$E/2V_L = \cos k_{\nu\mu} + \cos\left(\frac{2\pi\nu}{N-1}\right) + \cos\left(\frac{2\pi\mu}{M-1}\right) \quad (5.4)$$

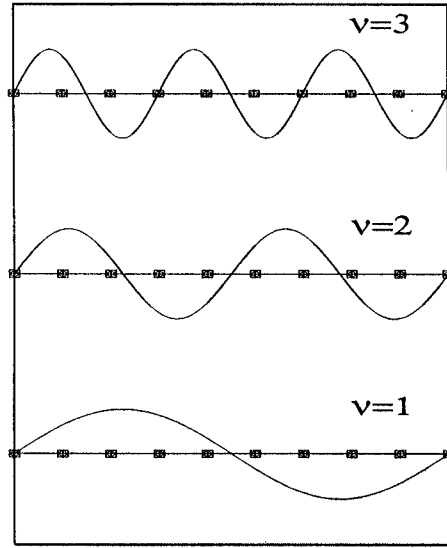


Figure 5.2: Some mode profiles along the finite section of a two-dimensional lead

The k label in the direction of motion of the electron depends on the particular mode labelled by $\{\nu\mu\}$ and the energy window too, depends on the mode:

$$-1 + \cos\left(\frac{2\pi\nu}{N-1}\right) + \cos\left(\frac{2\pi\mu}{M-1}\right) \leq E/2V_L \leq 1 + \cos\left(\frac{2\pi\nu}{N-1}\right) + \cos\left(\frac{2\pi\mu}{M-1}\right) \quad (5.5)$$

The figure 5.2 shows some cross-sectional profiles of the travelling modes in a two dimensional lead with nine atoms along the finite cross-section. Since the modes are eigenfunctions of the lead Hamiltonian, the shape of the cross-sections remain unchanged. An alternative boundary condition is to use the condition that the wavefunction of the travelling modes vanish on the faces.

In case the shapes of the scatterer and the leads do not match, that is, if the number of sites on their cross-sections are different, a slight difficulty arises. The

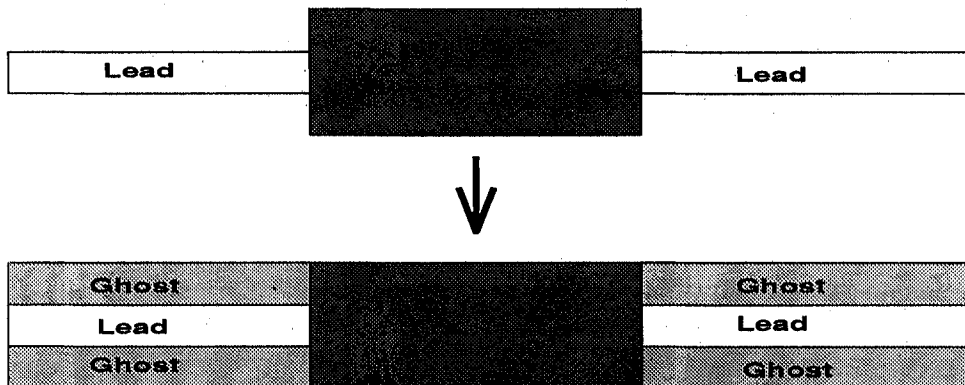


Figure 5.3: An illustration of 'ghost' leads

trick is to append *ghost* leads on either side of the faces and make the wavefunction vanish on these. There are hence $N' \times M'$ leads and as before $N \times M$ distinct non-trivial modes. Figure 5.3 illustrates this.

The wavefunction in this case is given by:

$$|k_{\mu\nu}, \mu, \nu\rangle = \sum_{n_1} \sum_{n_2} \sum_{n_3} \Psi_{n_1, n_2, n_3}(k_{\nu\mu}, \nu, \mu) |n_1, n_2, n_3\rangle$$

such that

$$\Psi_{n_1, n_2, n_3}(k_{\nu\mu}, \nu, \mu) = N_{\mu\nu} \exp(\pm i k_{\nu\mu} n_1) \sin\left(\frac{2\pi\nu}{N+1} n_2\right) \sin\left(\frac{2\pi\mu}{M+1} n_3\right) \quad (5.6)$$

here $n_2, n_3 = 0, 1, \dots, (N+1)(M+1)$, but $\mu, \nu = 1, 2, \dots, N(M)$. It is easy to check that the dispersion relation remains the same.

Let us now consider the modes to be labelled by a composite index $\xi = \{k_{\mu\nu}, \mu, \nu\}$. The first thing we note is that the mode wavefunctions $|k_\xi, \xi\rangle$ are eigenfunctions of the lead Hamiltonian. Within the energy window, k_ξ is real, so the modes propagate without attenuation or decay along the x-direction in the leads.

Moreover their profiles in the y-z direction remain unchanged in shape and are simply modulated by the exponential function along the x-direction. Figure 5.4 illustrates one of these propagating modes travelling along a lead.

From equations (5-3) we write, for a particular mode labelled by ξ

$$\begin{aligned} |\xi\rangle &= \sum_{n_1} \sum_{n_2} \sum_{n_3} \frac{1}{\sqrt{2\pi}} \exp(ik_\xi n_1) F(\xi, n_2, n_3) |n_1, n_2, n_3\rangle \\ &= \sum_{n_1} \frac{1}{\sqrt{2\pi}} \exp(ik_\xi n_1) |n_1, \xi\rangle \end{aligned} \quad (5.7)$$

The normalization factors have been absorbed into the definition of $F(\xi, n_2, n_3)$. Using the orthogonality of the exponential and Fourier like functions,

$$\langle \xi' | \xi \rangle = \delta_{\xi, \xi'}$$

5.2.2 Mode-mode scattering

When this travelling mode enters the scatter, the Hamiltonian inside is :

$$H = \sum_{\underline{n}} \sum_{\underline{\eta}} V(\underline{n}, \underline{n} + \underline{\eta}) (|\underline{n}\rangle \langle \underline{n} + \underline{\eta}| + |\underline{n} + \underline{\eta}\rangle \langle \underline{n}|) \quad (5.8)$$

Here $\underline{\eta}$ are the nearest neighbour vectors in the scatterer and $\underline{n} = \{n_1, n_2, n_3\}$. Now, looking at the effect of the scatter Hamiltonian acting on a lead mode, we immediately see that within the scatterer these lead modes do not propagate without change of cross-sectional shape :

$$H |\xi\rangle = \sum_{\underline{n}} \exp(ik_\xi n_1) F(\xi, n_2, n_3) \left[\sum_{\underline{\eta}} V(\underline{n}, \underline{\eta}) |\underline{n} + \underline{\eta}\rangle \right]$$

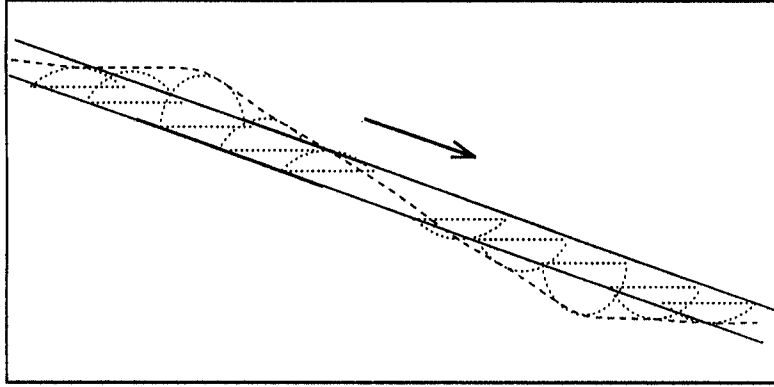


Figure 5.4: A mode propagating along a lead

We can now change the label $\underline{n} + \underline{\eta}$ to \underline{n}' . Take an example, for a cubic scatterer, there are six nearest neighbour vectors (± 100) , (0 ± 10) and (00 ± 1) and :

$$\begin{aligned}
 H |n_1, \xi\rangle &= \sum_{n_2} \sum_{n_3} F(\xi, n_2, n_3) \left[V^{(1)}(\underline{n}) |n_1 + 1, n_2, n_3\rangle + \dots \right. \\
 &\quad + V^{(2)}(\underline{n}) |n_1 - 1, n_2, n_3\rangle + \dots \\
 &\quad + \left\{ V^{(3)}(\underline{n}) \exp\left(\frac{2\pi i\nu}{N-1}\right) + V^{(4)}(\underline{n}) \exp\left(-\frac{2\pi i\nu}{N-1}\right) + \dots \right. \\
 &\quad \left. \left. + V^{(5)}(\underline{n}) \exp\left(\frac{2\pi i\mu}{M-1}\right) + V^{(6)}(\underline{n}) \exp\left(-\frac{2\pi i\mu}{M-1}\right) \right\} |n_1, n_2, n_3\rangle \right]
 \end{aligned}$$

Define,

$$\begin{aligned}
 V^{(1)}(n_1, n_2, n_3) F(\xi, n_2, n_3) &= \sum_{\xi'} A_{\xi\xi'}^{(1)}(n_1) F(\xi', n_2, n_3) \\
 V^{(2)}(n_1, n_2, n_3) F(\xi, n_2, n_3) &= \sum_{\xi'} A_{\xi\xi'}^{(2)}(n_1) F(\xi', n_2, n_3) \\
 \left\{ V^{(3)}(\underline{n}) \exp\left(\frac{2\pi i\nu}{N-1}\right) + V^{(4)}(\underline{n}) \exp\left(-\frac{2\pi i\nu}{N-1}\right) + \dots \right. \\
 \left. + V^{(5)}(\underline{n}) \exp\left(\frac{2\pi i\mu}{M-1}\right) + V^{(6)}(\underline{n}) \exp\left(-\frac{2\pi i\mu}{M-1}\right) \right\} F(\xi, n_2, n_3) \\
 &= \Phi(\xi, n_1, n_2, n_3) F(\xi, n_2, n_3) = \sum_{\xi'} A_{\xi\xi'}^{(3)}(n_1) F(\xi', n_2, n_3)
 \end{aligned}$$

Using the orthonormality of the Fourier functions,

$$\begin{aligned} A_{\xi\xi'}^{(1)}(n_1) &= \sum_{n_2} \sum_{n_3} V^{(1)}(n_1, n_2, n_3) F(\xi, n_2, n_3) F^*(\xi', n_2, n_3) \\ A_{\xi\xi'}^{(2)}(n_1) &= \sum_{n_2} \sum_{n_3} V^{(2)}(n_1, n_2, n_3) F(\xi, n_2, n_3) F^*(\xi', n_2, n_3) \\ A_{\xi\xi'}^{(3)}(n_1) &= \sum_{n_2} \sum_{n_3} \Phi(\xi, n_1, n_2, n_3) F(\xi, n_2, n_3) F^*(\xi', n_2, n_3) \end{aligned}$$

Thus,

$$H |n_1, \xi\rangle = \sum_{\xi'} \left\{ A_{\xi\xi'}^{(1)}(n_1) |n_1 + 1, \xi'\rangle + A_{\xi\xi'}^{(2)}(n_1) |n_1 - 1, \xi'\rangle + A_{\xi\xi'}^{(3)}(n_1) |n_1, \xi'\rangle \right\} \quad (5.9)$$

From the above equations it immediately follows that if all the Hamiltonian matrix elements are V_L then any mode wavefunction

$$|\xi\rangle = \frac{1}{\sqrt{2\pi}} \sum_{n_1} \exp(ik_\xi n_1) |n_1, \xi\rangle$$

is an eigenfunction of H with eigenvalue

$$2V_L \left\{ \cos(k_\xi) + \cos\left(\frac{2\pi\nu}{N-1}\right) + \cos\left(\frac{2\pi\mu}{M-1}\right) \right\} = E_\xi$$

However, once inside the scatterer, the off-diagonal elements of the Hamiltonian in a mode-mode basis (equation 5.9) causes scattering into other modes, so that the pure mode cannot propagate in the scatterer with its cross-sectional shape intact.

5.2.3 Vector recursion in a mode basis

In terms of the mode-mode representation of the scatterer Hamiltonian, the problem has been reduced to one with multiple individual leads. We may now apply the vector recursion method, described earlier, to obtain the scattering S-matrix and consequently the transmittance and reflectance.

We now set up the equations for the scattering problem. Suppose an incoming pure mode (labelled by ξ) travels through the left lead, meets the scatterer and a mixed mode reflected wave travels back along the left lead and another mixed mode transmitted wave comes out into the right lead and then propagates in it. The waves in the left and right leads in this problem are :

$$\begin{aligned}
 |\mathbf{Left}(\xi)\rangle &= \sum_{n_1} \sum_{\xi'} [\delta_{\xi\xi'} \exp ik'_\xi n_1 + r_{\xi\xi'} \exp(-ik'_\xi n_1)] |n_1, \xi'\rangle \\
 |\mathbf{Right}(\xi)\rangle &= \sum_{n_1} \sum_{\xi'} t_{\xi\xi'} \exp(-ik'_\xi n_1) |n_1, \xi'\rangle
 \end{aligned} \tag{5.10}$$

We now turn to the vector recursion of Godin and Haydock on the scatter itself. As discussed earlier, the aim of this method is to obtain the scattering S-matrix of the sample. The representations of the set of kets $\{|\mathbf{Left}(\xi)\rangle\}$ and $\{|\mathbf{Right}(\xi)\rangle\}$ are now lumped together in column vectors of length $2N \times M$ as follows :

$$\mathbf{K}^{n_1} = \begin{pmatrix} |\langle n_1 | \mathbf{Left}(\xi_1) \rangle \\ |\langle n_1 | \mathbf{Left}(\xi_2) \rangle \\ \vdots \\ |\langle n_1 | \mathbf{Left}(\xi_{NM}) \rangle \\ |\langle n_1 | \mathbf{Right}(\xi_1) \rangle \\ |\langle n_1 | \mathbf{Right}(\xi_2) \rangle \\ \vdots \\ |\langle n_1 | \mathbf{Right}(\xi_{NM}) \rangle \end{pmatrix}$$

A new basis is calculated recursively in which the sample Hamiltonian becomes block tridiagonal i.e. if we partition the sample Hamiltonian into matrix blocks of size $2NM \times 2NM$ then only the diagonal and sub-diagonal blocks are nonzero. The lead Hamiltonian is kept unchanged. The first element Ψ_1 of this basis is chosen to be

$$\Psi_1 = \begin{bmatrix} u_1^L \\ u_2^L \\ \vdots \\ u_{NM}^L \\ u_1^R \\ u_2^R \\ \vdots \\ u_{NM}^R \end{bmatrix}$$

Subsequent elements of the basis are generated from the following relations:

$$\begin{aligned} \mathbf{B}_2^\dagger \Psi_2 &= (\hat{\mathbf{H}} - \mathbf{A}_1) \Psi_1 \\ \mathbf{B}_{n+1}^\dagger \Psi_{s+1} &= (\hat{\mathbf{H}} - \mathbf{A}_n) \Psi_s - \mathbf{B}_n \Psi_{s-1} \end{aligned} \quad (5.11)$$

where $n \geq 2$. The original basis of the sample containing N_s orbitals is represented

by N_s now vectors of size N_s and the new basis is represented by matrices of size $2NM \times N_s$. A_n 's and B_n 's are $2NM \times 2NM$ matrices,

$$\begin{aligned}
 \mathbf{A}_s &= \Psi_s^\dagger \hat{\mathbf{H}} \Psi_s \\
 \mathbf{B}_s &= \Psi_{s+1}^\dagger \hat{\mathbf{H}} \Psi_s \\
 \mathbf{B}_1 &= V_L \mathbf{I}
 \end{aligned} \tag{5.12}$$

In the mode basis the boundary conditions satisfied by the set $\{\mathbf{K}^s\}$ are :

$$\mathbf{K}^{(0)} = \begin{pmatrix} 1 + \sum_{\xi'} r_{1,\xi'} \\ 1 + \sum_{\xi'} r_{2,\xi'} \\ \vdots \\ 1 + \sum_{\xi'} r_{NM,\xi'} \\ \sum_{\xi'} t_{1,\xi'} \\ \sum_{\xi'} t_{2,\xi'} \\ \vdots \\ \sum_{\xi'} t_{NM,\xi'} \end{pmatrix} \tag{5.13}$$

$$\mathbf{K}^{(1)} = \begin{pmatrix} \exp(ik\xi_1) + \sum_{\xi'} r_{1,\xi'} \exp(-ik\xi') \\ \exp(ik\xi_2) + \sum_{\xi'} r_{2,\xi'} \exp(-ik\xi') \\ \vdots \\ \exp(ik\xi_{NM}) + \sum_{\xi'} r_{NM,\xi'} \exp(-ik\xi') \\ \sum_{\xi'} t_{1,\xi'} \exp(ik\xi') \\ \sum_{\xi'} t_{2,\xi'} \exp(ik\xi') \\ \vdots \\ \sum_{\xi'} t_{NM,\xi'} \exp(ik\xi') \end{pmatrix} \tag{5.14}$$

where $1, 2, \dots, L$ are the modes in the incoming lead and $L+1, L+2, \dots, 2L$ are the modes in the outgoing lead, with $L = NM$. $r_{\nu\mu}$ represents the reflection coefficient of the electronic wavelet which enters the sample in the mode ν and after getting scattered in the sample, gets reflected into the mode μ into incoming lead, while

$t_{\nu\mu}$ represents the transmission coefficient of the electronic wavelet which enters the sample in the mode ν and after getting scattered in the sample, gets transmitted into a mode μ in the outgoing lead.

The wavefunction amplitudes are given by :

$$\mathbf{K}^{(s)} = \mathbf{X}^s \mathbf{K}^{(0)} + \mathbf{Y}^s \mathbf{K}^{(1)} \quad (5.15)$$

where $\{\mathbf{X}^s\}$ and $\{\mathbf{Y}^s\}$ are solution of the same recurrence relation as the $\{\mathbf{K}^{(s)}\}$ but with boundary conditions $\mathbf{X}^0 = \mathbf{I}$, $\mathbf{X}^1 = \mathbf{0}$ and $\mathbf{Y}^0 = \mathbf{0}$, $\mathbf{Y}^1 = \mathbf{I}$. Since the change of basis from site to mode does not change the rank of the underlying Hilbert space,

$$\mathbf{K}^{(2NM+1)} = \mathbf{X}^{2NM+1} \mathbf{K}^{(0)} + \mathbf{Y}^{2NM+1} \mathbf{K}^{(1)} = \mathbf{0} \quad (5.16)$$

Interchanging the incoming and outgoing leads we get another set of solutions.

Clubbing them together we obtain the **S**-matrix :

$$\mathbf{S} = -\left(\mathbf{X}^{2NM+1} + \mathbf{Y}^{2NM+1} \mathbf{E}^*\right)^{-1} \left(\mathbf{X}^{2NM+1} + \mathbf{Y}^{2NM+1} \mathbf{E}\right) \quad (5.17)$$

where

$$\mathbf{E} = \begin{pmatrix} \exp(ik_{\xi_1}) & 0 & \dots & 0 \\ 0 & \exp(ik_{\xi_2}) & \dots & 0 \\ & \ddots & & \\ 0 & 0 & \exp(ik_{\xi_1}) & 0 \\ & & \ddots & \\ 0 & 0 & \dots & \exp(ik_{\xi_{NM}}) \end{pmatrix}$$

In the absence of external magnetic fields the **S** matrix is symmetric and the reflectance and transmittance are given by :

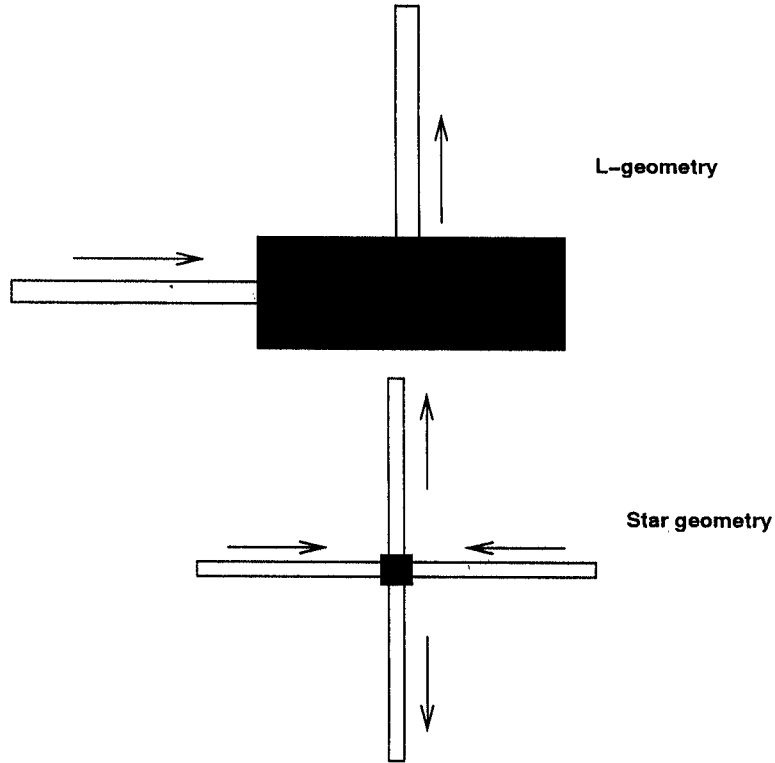


Figure 5.5: Scattering in a L-geometry and a Star-geometry

$$R(E) = \left| (1/NM) \sum_{\xi} \sum_{\xi'} r_{\xi\xi'}(E) \right|^2 \quad (5.18)$$

and

$$T(E) = \left| (1/NM) \sum_{\xi} \sum_{\xi'} t_{\xi\xi'}(E) \right|^2 \quad (5.19)$$

The Landauer formula offers the expression for conductance (in units of universal conductance) as :

$$G = \frac{T(E_F)}{R(E_F)} \quad (5.20)$$

5.3 Discussion

The method discussed above has the distinct advantage that the states which must be known exactly to match the boundary conditions are included *a priori* in the basis. This is why the method can also be applied to the case where some of the leads are attached at intermediate positions of the sample and not necessarily at the two ends. Problems where the electronic waves enter the sample in perpendicular directions (L-geometry) or the four-lead star geometry can be tackled within this technique.

It should be noted that resistance is a non-local object in the mesoscopic regime and depends on where the leads are attached to the scatterer (Gopar *et al* (1994), Tarucha *et al* (1992)). Note also that there is no assumption of V_{ij} to be short-ranged. We can begin with long-ranged overlaps and set about to block diagonalize the Hamiltonian using the Vector Recursion.

Bibliography

- Abrahams E., Anderson P.W., Licciardello D.C. and Ramakrishnan T.V., *Phys. Rev. Lett.* **42** 673 (1979)
- Al'tschuler B.L. and Aronov A.G., in *Electron-electron interactions in disordered systems* eds. A.L. Efros and M. Pollok (Elsevier, Amsterdam) (1985)
- Al'tschuler B.L. and Shklovskii B.I., *Sov. Phys.- JETP* **64** 127 (1986)
- See *Mesoscopic Phenomenon in Solids* edited by Al'tschuler B. L., Lee P. A. and Webb R.A. (North Holland, Amsterdam) (1991)
- Anderson P.W., *Phys. Rev.* **109** 1492 (1958)
- Azbel M., *Phys. Rev.* **B27** 3852 (1983) ; *Phys. Rev.* **B28** 4106 (1983) ; *Phil. Mag.* **nB50** 229 (1984)
- Azbel M.Y. and Soven P., *Phys. Rev. Lett.* **49** 751 (1982) ; *Phys. Rev.* **B27** 831 (1983)
- Pendry J.B., *J. Phys. C: Solid State Phys.* **20** 733 (1987).
- Baranger H.U. and Stone A.D., *Phys. Rev.* **B40** 8169 (1989)
- Basu C., Mookerjee A., Sen A.K. and Thakur P.K., *J. Phys.: Condens. Matter* **3** 6041 (1991)
- Basu C., Mookerjee A., Sen A.K. and Thakur P.K., *J. Phys.: Condens. Matter* **3** 9055 (1991)
- Basu C and Thakur P.K., *Physica* **A217** 289 (1995)
- Bellani V., Diez E., Hey R., Toni L., Tarricone L., Parravicini G.B., Dominguez-Adame F. and Gómez-Alacalá R., *Phys. Rev. Lett.* **82** 2159 (1999)
- Bergmann G., *Phys. Rev.* **B28** 2914 (1983)

- Berthod C., Gagel F. and Mashke K., *Phys. Rev.* **B50**, 18299 (1994).
- Borland R.E., *Proc. Phys. Soc.* **77** 705 (1961) ; **78** 926 (1961); Borland R.E., *Proc. Roy. Soc.* **A274** 529 (1963) ; Borland R.E., *Prog. Phys. Soc.* **83** 1027 (1964)
- Brody T.A., Flores J., French J.B., Mello P.A. and Pandey A. and Wong S.S.M., *Rev. Mod. Phys.* **53** 385 (1981)
- Buot F.A., *Phys Rep* **234 (2-3)** 73 (1993)
- Büttiker M., *Phys. Rev. Lett.* **57** 1761 (1986)
- Büttiker M., Imry Y., Landauer R., and Pinhas S. *Phys. Rev.* **B31** 6207 (1985)
- Chhabra A. and Jensen R.V., *Phys. Rev. Lett.* **62** 1327 (1989)
- Chakraborti A., Karmakar S. and Moitra R.K., *Phys. Rev. Lett.* **74** 1403 (1995)
- Chen X. and Xiong S., *Phys. Lett.* **A179** 217 (1993)
- Dasgupta I., Saha T. and Mookerjee A., *J. Phys.: Condens. Matter* **4** 7865 (1992)
- Dasgupta I., Saha T. and Mookerjee A., *Phys. Rev.* **B50** 4867 (1994)
- Datta P.K., Giri D. and Kundu K., *Phys. Rev.* **B47** 10727 (1993)
- Datta P.K., Giri D. and Kundu K., *Phys. Rev.* **B48** 16347 (1993)
- Ducker H., Struck M., Koslowski T and Von Niessen W., *Phys. Rev.* **B46** 13078 (1992)
- Dunlap D.H., Kundu K. and Phillips P., *Phys. Rev.* **B40** 10999 (1989)
- Dunlap D.H., Wu H.L. and Phillips P., *Phys. Rev. Lett.* **65** 88 (1990)
- Dyson F.J., *J. Math. Phys.* **3** 140; 157; 166 (1962)
- Evangelou S.N., Xiong S.J. and Economou E.N., *Phys. Rev.* **B54** 8469 (1996)
- Fisher D.S. and Lee P.E., *Phys. Rev.* **B23** 6851 (1981)
- Fujiwara T., Kohmoto M. and Tokihiro T., *Phys. Rev.* **B40** 7413 (1989)
- Gangopadhyay S. and Sen A.K., *J. Phys.: Condens. Matter* **4** 9939 (1992)
- Giri D., Datta P.K. and Kundu K., *Phys. Rev.* **B48** 14113 (1993)
- Godin T.J. and Haydock R., *Phys. Rev.* **B38** 5237 (1988)
- Godin T.J. and Haydock R., *EuroPhys. Lett*, **14** 137 (1991).

- Gopar V.A., Martinez M. and Mello P.A., *PR* **B50** 2502 (1994).
- Greenwood A.D., *Proc. Phys. Soc.* **71** 585 (1958)
- Grussbach H. and Schreiber M., *Phys. Rev.* **48** 6650 (1993)
- Haque A. and Khandker A. N., *Phys. Rev.* **B54** 5016 (1996).
- Heinrichs J., *Phys. Rev.* **51** 5699 (1995)
- Hilborn R., *Chaos and Nonlinear Dynamics* Oxford University Press (1994)
- Hilke M., *J. Physique* **A27** 4773 (1994)
- Imry Y., in *Directions in Condensed Matter Physics* eds. G. Grinstein and G. Mazenko (World Scientific, Singapore) (1986)
- Ishii K., *Prag. Theor. Phys. Suppl* **53** 77 (1973)
- Kawamura T. and Leburton J.P., *Phys. Rev.* **B48** 8857 (1993)
- Kubo R., *Can. J. Phys.* **34** 1274 (1956) ; *J. Phys. Soc. (Japan)* **12** 570 (1957)
- Landauer R., *Philos. Mag.* **21** 863 (1970)
- Leng M. and Lent C.S., *Phys. Rev. Lett.* **71** 137 (1993)
- Macia E. and Dominguez A.F., *Phys. Rev. Lett.* **76** 2957 (1996)
- Mandelbrot B. B., *The Fractal Geometry of Nature* (W.H. Freeman, San Francisco) (1982) ; *Phys. Scr.* **32**, 257 (1985)
- Mehta M.L., *Random matrices and the statistical theory of energy levels* (Academic Press, New York) (1967)
- Mello P.A., *Phys. Rev. Lett.* **60** 1089 (1988)
- Mitin V., Kochelap V.A. and Strosio M.A., *Quantum Heterostructures* (Cambridge University Press) (1999)
- Mitra T. and Thakur P.K., *Phys. Rev.* **B53** 9895 (1996)
- Mitra T. and Thakur P.K., *Int. J. Mod. Phys.* **B12** 1773 (1998)
- Mott N.F. and Twose W.D., *Adv. Phys.* **10** 107 (1961)
- Muttalib K.A., Picard J.L. and Stone A.D., *Phys. Rev. Lett.* **59** 2475 (1987)
- Nikolic K. and Mackinhon A, *Phys. Rev.* **B50** 110081 (1994).

- Pendry J.B., *J. Phys. C: Solid State Phys.* **20** 733 (1987)
- Phillips P., Wu H.L. and Dunlap D., *Mod. Phys. Lett.* **B4** (1990)
- Phillips P. and Wu H.L., *Science* **252** 1805 (1991)
- Progodin V.N. and Efetov K.B., *Phys. Rev. Lett.* **70** 2932 (1993)
- Saha T., Dasgupta I. and Mookerjee A., *Phys. Rev.* **B50** 4867 (1994)
- Ramakrishnan T.V. and Lee P.A., *Rev. Mod. Phys.* **57** 287 (1985)
- Richter K., Ullmo D. and Jalebert R.A. , *Phys. Rev.* **B54** R5219 (1996).
- Römer R.A. and Schreiber M., *Phys. Rev. Lett.* **78** 515 (1997)
- Sanchez A., *Phys. Rev.* **B49** 147 (1994)
- Schreiber M. and Grussbach H., *Phys. Rev. Lett.* **67** 607 (1991).
- Sil S., Karmakar S.N., Moitra R.K. and Chakraborty A., *Phys. Rev.* **B48** 4192 (1993)
- Singha Deo P. and Jayannavar A.M. , *Phys. Rev.* **B50**, 11629 (1994).
- Shepelyanski D.L., *Phys. Rev. Lett.* **73** 2607 (1994)
- Sols F., Macucci M., Ravaioli V., and Hess K., *J. Appl. Phys.* **66(8)** 3892 (1989)
- Soukoulis C.M., Velgakis M.J. and Economou E.N., *Phys. Rev.* **B50** 5110 (1994)
- Stafstrom S., *Phys. Rev.* **B51** 4137 (1995)
- Stone A.D. and Szafer A., *IBM J. Res. Dev.* **32** 384 (1988)
- Tarucha S., Hirayama Y., Saku T. and Horikoshi Y., in *Nanostructures and Mesoscopic systems* edited by W.P. Kirk and M.A. Reed, (Academic Press Inc., 1992)
- Thakur P.K., Basu C. and Mookerjee A., *J. Phys.: Condens. Matter* **4** 6095 (1992)
- Thakur P.K. and Mitra T., *J. Phys.: Condens. Matter* **9** 8985 (1997)
- Vacek K., Okiji A. and Kasai H., *Phys. Rev.* **B48** 11412 (1993).
- van Wees B.J., van Howten H., Beenakker C.W.J., Williamson J.G., Kouwenhoven L.P., van der Marel D. and Poxon C.T., *Phys. Rev. Lett.* **60** 848 (1988)
- Washburn S. and Webb R.A., *Adv Phys* **35** 375 (1986)
- Weisbuch C. and Vinter B., *Quantum Semiconductor Structures* (1991)
Academic Press Inc.

- Wharam D.A., Thornton T.J., Newbury R., Pepper M., Ajmed H., Frost J.E.F., Hasko D.G., Peacock D.C., Ritchie D.A. and Jones G.A.C., *J. Phys. C: Solid State Phys.* **21** L209 (1988)
- Wu H.L. and Phillips P., *Phys. Rev. Lett.* **66** 1366 (1991)
- Wu H.L., Goff W. and Phillips P., *Phys. Rev.* **B45** 1623 (1992)
- Yakubo K. and Goto Y., *Phys. Rev.* **B54** 13432 (1996)
- Zanon N. and Pichard J.L., *J. Phys. (France)* **49** 907 (1988)